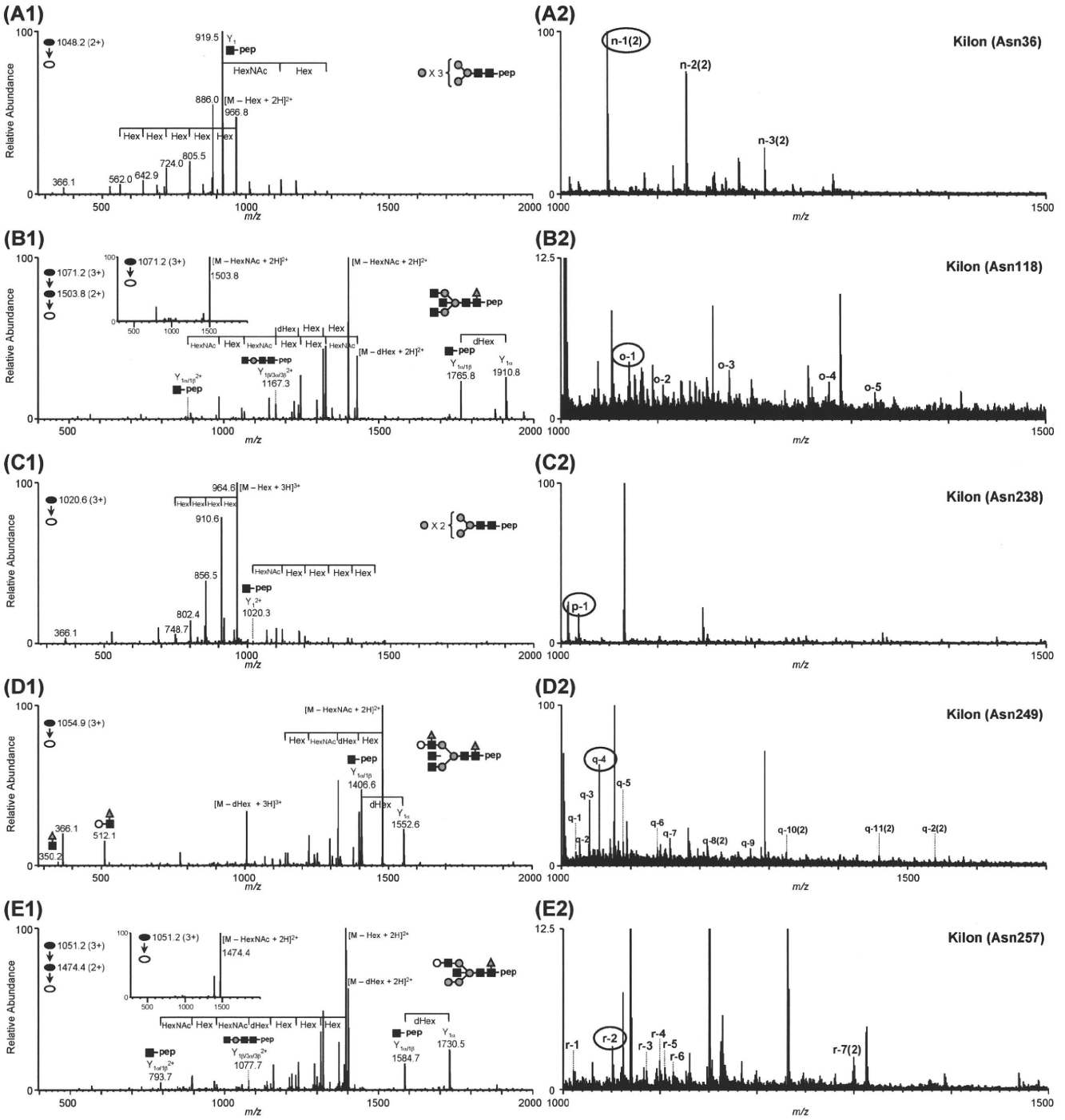

FIGURE 8: MS spectra of Kilon glycopeptides. (A1) MS/MS spectra of glycopeptide GAWLN^{36}R; elution position, 3; precursor ion, $[M + 2H]^{2+}$ (*m/z* 1048.2). (A2) Integrated mass spectrum obtained from position 3. (B1) MS/MS and MS/MS/MS spectra of glycopeptide GTN^{118}VTLTCLATGKPE; elution position, 16; precursor ion, $[M + 3H]^{3+}$ (*m/z* 1071.2). (B2) Integrated mass spectrum at position 16. (C1) MS/MS spectrum of glycopeptide LFNGQQGIIIQN^{238}FSTR; elution position, 22; precursor ion, $[M + 3H]^{3+}$ (*m/z* 1020.6). (C2) Integrated mass spectrum at position 22. (D1) MS/MS spectrum of glycopeptide SILTVTN^{249}VTQE; elution position, 17; precursor ion, $[M + 3H]^{3+}$ (*m/z* 1054.9). (D2) Integrated mass spectrum at position 17. (E1) MS/MS and MS/MS/MS spectra of glycopeptide HFGN^{257}YTCVAANK; elution position, 10; precursor ion, $[M + 3H]^{3+}$ (*m/z* 1051.2). (E2) Integrated mass spectrum at position 10. Symbols are as in Figure 9.

HexNAc-(Hex-)(NH_2Et-PO_4-)Man3, and HexNAc-(NH_2Et-PO_4-)Man3, respectively. The existence of two isomers was suggested in peak N2 by the presence of two different MS/MS spectra at different elution times (Table 2).

Glycosylation Analysis of Kilon. Kilon has six potential N-glycosylation sites at Asn36, -118, -238, -249, -257, and -270. The predicted linkage site of GPI is Gly287. The typical MS/MS spectra and the integrated mass spectra of the glycopeptides containing Asn36, -118, -238, -249, and -257 are shown in panels A1−E1 and A2−E2 of Figure 8, respectively. The MS/MS spectra of the glycopeptide containing both Asn270 and Gly287 could not be picked out from the MS data.

(i) Asn36. Panel A1 of Figure 8 shows one of the MS/MS spectra acquired at position 3. This glycopeptide was identified as GAWLN^{36}R with Man-6 based on Y_1 ion and the monosaccharide composition. Other glycans at Asn36 were estimated as Man-5, -7, and -8 from the existence of

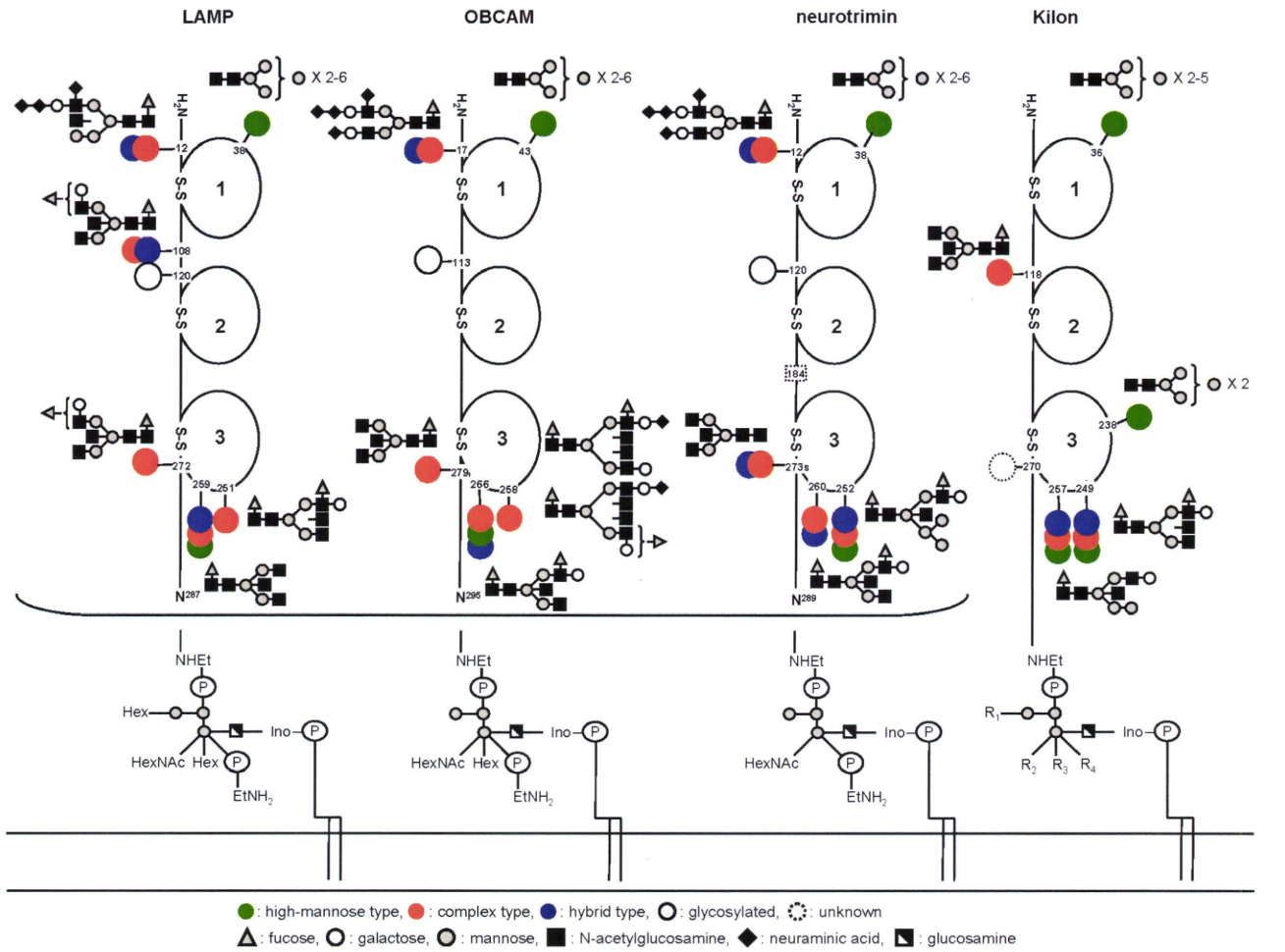

FIGURE 9: Summary of glycosylation of IgLON family proteins.

molecular ions with 81 *m/z* units intervals in the integrated mass spectrum (peaks n-1−3 in panel A2 of Figure 8) (Table 1N).

(ii) Asn118. As shown in panel B1 of Figure 8, the MS/MS/MS spectrum acquired at position 16 contained $Y_{1\alpha/1\beta}$, which suggested that the peptide portion is GTN[118]VTLTCLATGKPE. The linkage of BA-2 was deduced from the monosaccharide composition ($dHex_1Hex_3HexNAc_5$), and $Y_{1\beta/3\alpha/3\beta}^{2+}$ and $Y_{1\alpha}$ (inset of panel B1 of Figure 8). Additionally, the linkage of $Le^{a/x}$ or antigen H-modified and/or bisected complex type was suggested by the integrated mass spectrum (peaks o-1−5 in panel B2 of Figure 8 and Table 1O).

(iii) Asn238. The MS/MS spectra of glycopeptides that contain Asn238 were picked out from positions 22 [LFNGQQGIIIQN[238]FSTR (panel C1 of Figure 8)], 21 (RLFNGQQGIIIQN[238]FSTR), and 19 (KRLFNGQQGIII-QN[238]FSTR). These MS/MS spectra and molecular ions appearing in the integrated mass spectrum revealed that the only carbohydrate structure at Asn238 was Man-5 (peak p-1 in panel C2 of Figure 8 and Table 1P). Together with the results of the database search analysis, in which nonglycosylated peptide LFNGQQGIIIQN[238]FSTR was identified, it was suggested that Man-5 was partly attached to Asn238 (Table 1P).

(iv) Asn249. Panel D1 of Figure 8 shows the representative MS/MS spectrum of glycopeptide SILTVTN[249]VTQE at position 17. The carbohydrate structure was characterized as a $Le^{a/x}$-modified and core-fucosylated complex type by the existence of the $Le^{a/x}$-related ions and $Y_{1\alpha}$. The integrated mass spectrum and alternative LC−MS^n with the C30 column (scan ranges of *m/z* 700−2000 and 1000−2000) suggested that Asn249 is glycosylated with $Le^{a/x}$ or antigen H-modified core-fucosylated hybrid- and complex-type oligosaccharides, BA-2, and Man-5 (peaks q-1−11 in panel D2 of Figure 8 and Table 1Q).

(v) Asn257. As shown in panel E1 of Figure 8, one of the glycopeptides eluted at position 10 was identified as HFGN[257]YTCVAANK linked by $dHex_1Hex_5HexNAc_4$ based on $Y_{1\alpha/1\beta}$ ion in the MS/MS/MS spectra and monoisotopic mass. The carbohydrate structure was characterized as a bisected- and core-fucosylated hybrid-type oligosaccharide based on the presence of $Y_{1\beta/3\alpha/3\beta}^{2+}$ and $Y_{1\alpha}$ (inset of panel E2 of Figure 8). Other major glycans were estimated as Man-5, $Le^{a/x}$-modified complex- and hybrid-type oligosaccharides, and BA-2 (peaks r-1−7 in panel E2 of Figure 8 and Table 1R).

DISCUSSION

The cell adhesion molecules in the central nervous system play an essential role in the differentiation of neuronal cells and formation of neural circuits. Although glycosylation on the cell adhesion molecules is known to regulate cell−cell interactions (*2*−*4*), their carbohydrate structures remain unknown due to the difficulty with respect to their isolation and the limited sample amounts. The glycans in the IgLON family proteins are considered to be implicated in the

formation of neural circuits, including migration of neuronal cells, axonal guidance, and fasciculation. However, the high degree of homology of their amino acid sequences makes it difficult to isolate them from each other and to analyze their carbohydrate structures in detail.

In this study, we performed a site-specific glycosylation analysis of LAMP, OBCAM, neurotrimin, and Kilon simultaneously using SDS−PAGE and LC−MS^n. Enriched GPI-linked proteins were separated by SDS−PAGE, and four target proteins were extracted from a gel piece together with other contaminating proteins. The protein mixture was digested and analyzed by the C30 and C18-LC−MS^n runs via MS, data-dependent MS in SIM by the FT ICR-MS, and data-dependent MS/MS and MS/MS/MS. A set of MS data consisting of the mass spectrum, the mass spectrum acquired by the FT ICR-MS in SIM mode, the data-dependently acquired MS/MS, and the MS/MS/MS spectra of a glycopeptide was selected from all MS data on the basis of the existence of the oligosaccharide characteristic oxonium ions in the MS/MS spectrum. The carbohydrate structure and peptide sequence were deduced from the carbohydrate-related ions and peptide-related ions in the product ion spectra. The structural assignment of the glycopeptide was confirmed by the accurate mass acquired on the FT ICR-MS. The b- and y-ions arising from the peptide backbone in the MS/MS/MS spectra were also used for the peptide assignment. The carbohydrate heterogeneity at each glycosylation site was characterized by integrating the mass spectra of the glycopeptides which yielded identical peptide-related ions. We successfully determined the site-specific glycosylation in LAMP, OBCAM, neurotrimin, and Kilon with the exception of Asn120 in LAMP, Asn113 in OBCAM, Asn120 in neurotrimin, and Asn270 in Kilon. We also demonstrated the structure of the GPI moiety using LC−MS^n equipped with a GCC. A set of data was picked out from all MS data by using GPI-characteristic ions, and the structure of GPI and the linkage site were deduced from the product ions in the MS/MS spectra. Three different structures are commonly found in LAMP, OBCAM, and neurotrimin.

Figure 9 illustrates the site-specific glycosylation in the four proteins. N-Glycosylation sites near the N-terminus in LAMP, OBCAM, and neurotrimin were commonly occupied with biantennary complex-type and hybrid-type oligosaccharides containing disialic acids. Oligosialic acids and disialic acids, which are found in several glycoproteins, including NCAM, are considered to regulate the cell−cell interaction by changing their degree of polymerization (*6*). Disialic acids at the near N-terminus in LAMP, OBCAM, and neurotrimin might regulate the cell−cell interaction in a manner similar to that of other glycosylated adhesion molecules.

The first domains in IgLON family proteins are commonly glycosylated with Man-5, -6, -7, -8, and -9. The linkage of high-mannose-type oligosaccharides is found in several Ig superfamily proteins, including L1, MAG, and P0 (*3*). Since Horstkorte et al. have reported that L1 binds to NCAM through oligomannosidic carbohydrates in L1 (*34*), the high-mannose-type oligosaccharide in IgLON family proteins could interact with certain biological molecules.

The third domains of all IgLON proteins were highly heterogeneous due to a linkage of diverse oligosaccharides, including BA-2, the $Le^{a/x}$ or $Le^{b/y}$ motif, and Man-5. BA-2, a bisected agalacto-complex type, is known as a brain-specific glycan and is much more abundant in mammalian brains than in other tissues (*35, 36*). Recently, the Na^+/K^+-ATPase $\beta 1$ subunit was identified as a GlcNAc-binding protein in the mouse brain (*37*). The Na^+/K^+-ATPase $\beta 1$ subunit is a potassium-dependent lectin which binds to GlcNAc-terminating oligosaccharides and is involved in neural cell interactions in a trans-binding fashion. A 74 kDa protein was suggested to be the GlcNAc-terminating glycan carrier protein binding to the Na^+/K^+-ATPase $\beta 1$ subunit. The linkage of BA-2 to IgLON family proteins implies that these proteins might be the ligand proteins for the Na^+/K^+-ATPase $\beta 1$ subunit.

Glycosylation in a great number of membrane glycoproteins remains largely unknown. This is mainly because the limited amount of available sample and the low solubility of glycoproteins make their isolation quite difficult. Our strategy, which includes enrichment of the target glycoproteins, separation by SDS−PAGE, and LC−MS^n of digests of a protein mixture, can be applied to the site-specific glycosylation analysis of various membrane glycoproteins.

ACKNOWLEDGMENT

We thank Dr. Masayuki Kubota and Morihiko Yoshida (Thermo Fisher Scientific K.K.) for their technical support.

REFERENCES

1. Walsh, F. S., and Doherty, P. (1997) Neural cell adhesion molecules of the immunoglobulin superfamily: Role in axon growth and guidance. *Annu. Rev. Cell Dev. Biol. 13*, 425–456.
2. Kleene, R., and Schachner, M. (2004) Glycans and neural cell interactions. *Nat. Rev. Neurosci. 5*, 195–208.
3. Krog, L., and Bock, E. (1992) Glycosylation of neural cell adhesion molecules of the immunoglobulin superfamily. *APMIS, Suppl. 27*, 53–70.
4. Schachner, M., and Martini, R. (1995) Glycans and the modulation of neural-recognition molecule function. *Trends Neurosci. 18*, 183–191.
5. Liedtke, S., Geyer, H., Wuhrer, M., Geyer, R., Frank, G., Gerardy-Schahn, R., Zahringer, U., and Schachner, M. (2001) Characterization of N-glycans from mouse brain neural cell adhesion molecule. *Glycobiology 11*, 373–384.
6. Rutishauser, U. (1996) Polysialic acid and the regulation of cell interactions. *Curr. Opin. Cell Biol. 8*, 679–684.
7. Kunemund, V., Jungalwala, F. B., Fischer, G., Chou, D. K., Keilhauer, G., and Schachner, M. (1988) The L2/HNK-1 carbohydrate of neural cell adhesion molecules is involved in cell interactions. *J. Cell Biol. 106*, 213–223.
8. Cho, T. M., Hasegawa, J., Ge, B. L., and Loh, H. H. (1986) Purification to apparent homogeneity of a μ-type opioid receptor from rat brain. *Proc. Natl. Acad. Sci. U.S.A. 83*, 4138–4142.
9. Funatsu, N., Miyata, S., Kumanogoh, H., Shigeta, M., Hamada, K., Endo, Y., Sokawa, Y., and Maekawa, S. (1999) Characterization of a novel rat brain glycosylphosphatidylinositol-anchored protein (Kilon), a member of the IgLON cell adhesion molecule family. *J. Biol. Chem. 274*, 8224–8230.
10. Levitt, P. (1984) A monoclonal antibody to limbic system neurons. *Science 223*, 299–301.
11. Pimenta, A. F., Zhukareva, V., Barbe, M. F., Reinoso, B. S., Grimley, C., Henzel, W., Fischer, I., and Levitt, P. (1995) The limbic system-associated membrane protein is an Ig superfamily member that mediates selective neuronal growth and axon targeting. *Neuron 15*, 287–297.
12. Schofield, P. R., McFarland, K. C., Hayflick, J. S., Wilcox, J. N., Cho, T. M., Roy, S., Lee, N. M., Loh, H. H., and Seeburg, P. H. (1989) Molecular characterization of a new immunoglobulin superfamily protein with potential roles in opioid binding and cell contact. *EMBO J. 8*, 489–495.
13. Struyk, A. F., Canoll, P. D., Wolfgang, M. J., Rosen, C. L., D'Eustachio, P., and Salzer, J. L. (1995) Cloning of neurotrimin

defines a new subfamily of differentially expressed neural cell adhesion molecules. *J. Neurosci. 15*, 2141–2156.
14. Brauer, A. U., Savaskan, N. E., Plaschke, M., Prehn, S., Ninnemann, O., and Nitsch, R. (2000) IG-molecule Kilon shows differential expression pattern from LAMP in the developing and adult rat hippocampus. *Hippocampus 10*, 632–644.
15. Gil, O. D., Zhang, L., Chen, S., Ren, Y. Q., Pimenta, A., Zanazzi, G., Hillman, D., Levitt, P., and Salzer, J. L. (2002) Complementary expression and heterophilic interactions between IgLON family members neurotrimin and LAMP. *J. Neurobiol. 51*, 190–204.
16. Hachisuka, A., Nakajima, O., Yamazaki, T., and Sawada, J. (2000) Developmental expression of opioid-binding cell adhesion molecule (OBCAM) in rat brain. *Brain Res. Dev. Brain Res. 122*, 183–191.
17. Miyata, S., Matsumoto, N., Taguchi, K., Akagi, A., Iino, T., Funatsu, N., and Maekawa, S. (2003) Biochemical and ultrastructural analyses of IgLON cell adhesion molecules, Kilon and OBCAM in the rat brain. *Neuroscience 117*, 645–658.
18. Zacco, A., Cooper, V., Chantler, P. D., Fisher-Hyland, S., Horton, H. L., and Levitt, P. (1990) Isolation, biochemical characterization and ultrastructural analysis of the limbic system-associated membrane protein (LAMP), a protein expressed by neurons comprising functional neural circuits. *J. Neurosci. 10*, 73–90.
19. Hachisuka, A., Yamazaki, T., Sawada, J., and Terao, T. (1996) Characterization and tissue distribution of opioid-binding cell adhesion molecule (OBCAM) using monoclonal antibodies. *Neurochem. Int. 28*, 373–379.
20. Wada, Y., Tajiri, M., and Yoshida, S. (2004) Hydrophilic affinity isolation and MALDI multiple-stage tandem mass spectrometry of glycopeptides for glycoproteomics. *Anal. Chem. 76*, 6560–6565.
21. Wuhrer, M., Hokke, C. H., and Deelder, A. M. (2004) Glycopeptide analysis by matrix-assisted laser desorption/ionization tandem time-of-flight mass spectrometry reveals novel features of horseradish peroxidase glycosylation. *Rapid Commun. Mass Spectrom. 18*, 1741–1748.
22. Satomi, Y., Shimonishi, Y., and Takao, T. (2004) N-Glycosylation at Asn(491) in the Asn-Xaa-Cys motif of human transferrin. *FEBS Lett. 576*, 51–56.
23. Zaia, J. (2004) Mass spectrometry of oligosaccharides. *Mass Spectrom. Rev. 23*, 161–227.
24. Wuhrer, M., Catalina, M. I., Deelder, A. M., and Hokke, C. H. (2007) Glycoproteomics based on tandem mass spectrometry of glycopeptides. *J. Chromatogr., B: Anal. Technol. Biomed. Life Sci 849*, 115–128.
25. Wuhrer, M., Koeleman, C. A., Hokke, C. H., and Deelder, A. M. (2005) Protein glycosylation analyzed by normal-phase nano-liquid chromatography-mass spectrometry of glycopeptides. *Anal. Chem. 77*, 886–894.
26. Harazono, A., Kawasaki, N., Kawanishi, T., and Hayakawa, T. (2005) Site-specific glycosylation analysis of human apolipoprotein B100 using LC/ESI MS/MS. *Glycobiology 15*, 447–462.
27. Sandra, K., Devreese, B., Van Beeumen, J., Stals, I., and Claeyssens, M. (2004) The Q-Trap mass spectrometer, a novel tool in the study of protein glycosylation. *J. Am. Soc. Mass Spectrom. 15*, 413–423.
28. Itoh, S., Kawasaki, N., Harazono, A., Hashii, N., Matsuishi, Y., Kawanishi, T., and Hayakawa, T. (2005) Characterization of a gel-separated unknown glycoprotein by liquid chromatography/multistage tandem mass spectrometry: Analysis of rat brain Thy-1 separated by sodium dodecyl sulfate-polyacrylamide gel electrophoresis. *J. Chromatogr., A 1094*, 105–117.
29. Bordier, C. (1981) Phase separation of integral membrane proteins in Triton X-114 solution. *J. Biol. Chem. 256*, 1604–1607.
30. Lisanti, M. P., Sargiacomo, M., Graeve, L., Saltiel, A. R., and Rodriguez-Boulan, E. (1988) Polarized apical distribution of glycosyl-phosphatidylinositol-anchored proteins in a renal epithelial cell line. *Proc. Natl. Acad. Sci. U.S.A. 85*, 9557–9561.
31. Itoh, S., Kawasaki, N., Ohta, M., and Hayakawa, T. (2002) Structural analysis of a glycoprotein by liquid chromatography-mass spectrometry and liquid chromatography with tandem mass spectrometry. Application to recombinant human thrombomodulin. *J. Chromatogr., A 978*, 141–152.
32. Kikuchi, M., Hatano, N., Yokota, S., Shimozawa, N., Imanaka, T., and Taniguchi, H. (2004) Proteomic analysis of rat liver peroxisome: Presence of peroxisome-specific isozyme of Lon protease. *J. Biol. Chem. 279*, 421–428.
33. Nakajima, O., Hachisuka, A., Takagi, K., Yamazaki, T., Ikebuchi, H., and Sawada, J. (1997) Expression of opioid-binding cell adhesion molecule (OBCAM) and neurotrimin (NTM) in *E. coli* and their reactivity with monoclonal anti-OBCAM antibody. *NeuroReport 8*, 3005–3008.
34. Horstkorte, R., Schachner, M., Magyar, J. P., Vorherr, T., and Schmitz, B. (1993) The fourth immunoglobulin-like domain of NCAM contains a carbohydrate recognition domain for oligomannosidic glycans implicated in association with L1 and neurite outgrowth. *J. Cell Biol. 121*, 1409–1421.
35. Chen, Y. J., Wing, D. R., Guile, G. R., Dwek, R. A., Harvey, D. J., and Zamze, S. (1998) Neutral N-glycans in adult rat brain tissue: Complete characterisation reveals fucosylated hybrid and complex structures. *Eur. J. Biochem. 251*, 691–703.
36. Nakakita, S., Natsuka, S., Ikenaka, K., and Hase, S. (1998) Development-dependent expression of complex-type sugar chains specific to mouse brain. *J. Biochem. 123*, 1164–1168.
37. Kitamura, N., Ikekita, M., Sato, T., Akimoto, Y., Hatanaka, Y., Kawakami, H., Inomata, M., and Furukawa, K. (2005) Mouse Na^+/K^+-ATPase β1-subunit has a K^+-dependent cell adhesion activity for β-GlcNAc-terminating glycans. *Proc. Natl. Acad. Sci. U.S.A. 102*, 2796–2801.

BI8009778

STEM CELLS

EMBRYONIC STEM CELLS/INDUCED PLURIPOTENT STEM CELLS

Efficient Adipocyte and Osteoblast Differentiation from Mouse Induced Pluripotent Stem Cells by Adenoviral Transduction

KATSUHISA TASHIRO,[a,b] MITSURU INAMURA,[a,b] KENJI KAWABATA,[b] FUMINORI SAKURAI,[b] KOICHI YAMANISHI,[a,c] TAKAO HAYAKAWA,[d,e] HIROYUKI MIZUGUCHI[a,b]

[a]Graduate School of Pharmaceutical Sciences, Osaka University, Osaka, Japan; [b]Laboratory of Gene Transfer and Regulation, National Institute of Biomedical Innovation, Osaka, Japan; [c]National Institute of Biomedical Innovation, Osaka, Japan; [d]Pharmaceutics and Medical Devices Agency, Tokyo, Japan; [e]Pharmaceutical Research and Technology Institute, Kinki University, Osaka, Japan

Key Words. Adenovirus • Differentiation • Gene expression • Induced pluripotent stem cells

ABSTRACT

Induced pluripotent stem (iPS) cells, which are generated from somatic cells by transducing four genes, are expected to have broad application to regenerative medicine. Although establishment of an efficient gene transfer system for iPS cells is considered to be essential for differentiating them into functional cells, the detailed transduction characteristics of iPS cells have not been examined. Previously, by using an adenovirus (Ad) vector containing the elongation factor-1α (EF-1α) and the cytomegalovirus enhancer/β-actin (CA) promoters, we developed an efficient transduction system for mouse embryonic stem (ES) cells and their aggregate form, embryoid bodies (EBs). In this study, we applied our transduction system to mouse iPS cells and investigated whether efficient differentiation could be achieved by Ad vector-mediated transduction of a functional gene. As in the case of ES cells, the Ad vector containing EF-1α and the CA promoter could efficiently transduce transgenes into mouse iPS cells. At 3,000 vector particles/cell, 80%–90% of iPS cells expressed transgenes by treatment with an Ad vector containing the CA promoter, without a decrease in pluripotency or viability. We also found that the CA promoter had potent transduction ability in iPS cell-derived EBs. Moreover, exogenous expression of a *PPARγ* gene or a *Runx2* gene into mouse iPS cells by an optimized Ad vector enhanced adipocyte or osteoblast differentiation, respectively. These results suggest that Ad vector-mediated transient transduction is sufficient to increase cellular differentiation and that our transduction methods would be useful for therapeutic applications based on iPS cells. STEM CELLS *2009;27:1802–1811*

Disclosure of potential conflicts of interest is found at the end of this article.

INTRODUCTION

Because embryonic stem (ES) cells, derived from the inner cell mass of mammalian blastocysts, can be cultured indefinitely in an undifferentiated state and differentiate into various cell types [1, 2], ES cells have been regarded as a potential source of specific cell populations for cell replacement therapy. However, there are two important issues that must be addressed before ES cells can be applied for regenerative medicine: one is the ethical issue about the use of embryos, and the other is the risk of immune rejection after transplantation. In 2006, Takahashi and Yamanaka [3] reported that ES cell-like pluripotent cells, designated as induced pluripotent stem (iPS) cells, could be generated from mouse skin fibroblasts by retroviral transduction of four genes (POU domain class 5 transcription factor 1 [*Oct-3/4*], SRY-box containing box 2 [*Sox2*], cellular myelocytomatosis oncogene [c-*Myc*], and Kruppel-like factor 4 [*Klf4*]). A recent study demonstrated that iPS cells possessed mostly the same characteristics as ES cells, such as global gene expression [4], DNA methylation [5], and histone modification [6]. Furthermore, iPS cells give rise to adult chimeric offspring and show competence for germline transmission [4–6]. Because iPS cells not only have the properties as described above but also can overcome the ethical concerns and problems with immune rejection and because human iPS cells can also be generated from somatic cells [7–10], they are expected to be applicable to regenerative medicine in place of ES cells.

To apply iPS cells to regenerative medicine, establishing methods for the differentiation of iPS cells into pure functional cells is indispensable. Among the many methods for promoting cellular differentiation, genetic manipulation is one of the most powerful techniques, because overexpression of a

Author contributions: K.T.: conception and design, collection and assembly of data, data analysis and interpretation, manuscript writing, final approval of manuscript; M.I.: collection and assembly of data, final approval of manuscript; K.K. and H.M.: conception and design, financial support, manuscript writing, final approval of manuscript; F.S., K.Y., and T.H.: conception and design, final approval of manuscript.

Correspondence: Hiroyuki Mizuguchi, Ph.D., Department of Biochemistry and Molecular Biology, Graduate School of Pharmaceutical Sciences, Osaka University, 1-6 Yamadaoka, Suita, Osaka 565-0871, Japan. Telephone: +81-6-6879-8185; Fax: +81-6-6879-8185; e-mail: mizuguch@phs.osaka-u.ac.jp Received November 25, 2008; accepted for publication April 23, 2009; first published online in STEM CELLS *EXPRESS* April 30, 2009. 1066-5099/2009/$30.00/0 doi: 10.1002/stem.108

differentiation-associated gene in the cells is considered to direct the cell fate from stem cells into functional cells. Many studies have reported that gene transfer into stem cells promoted their differentiation into functional differentiated cells, including hematopoietic cells [11], pancreatic cells [12], and neurons [13].

Adenovirus (Ad) vectors are some of the most efficient gene delivery vehicles and have been widely used in both experimental studies and clinical trials [14, 15]. Ad vectors are an attractive vehicle for gene transfer because they are easily constructed, can be prepared in high titers, and provide efficient transduction in both dividing and nondividing cells. We have developed efficient methods for Ad vector-mediated transduction into mouse ES cells and their aggregate form, embryoid bodies (EBs) [16, 17]. We also showed that adipocyte differentiation from mouse ES cells was markedly promoted by use of the Ad vector for transient transduction of the peroxisome proliferator-activated receptor γ (*PPAR*γ) gene [17], which is known to play essential roles in adipogenesis [18, 19].

Because our transduction method using an optimized Ad vector was effective for enhancing the differentiation of mouse ES cells into target cells, we attempted to apply this system to mouse iPS cells and examined whether the adipocyte and osteoblast differentiation potential of mouse iPS cells could be increased by using Ad vector. In all studies, mouse ES cells were used as a control for comparison with mouse iPS cells. By comparing the promoter activity in mouse iPS cells, we successfully developed a suitable Ad vector for gene transfer into mouse iPS cells. We also found that adipocyte and osteoblast differentiation from mouse iPS cells could be facilitated by Ad vector-mediated transient transduction of a *PPAR*γ gene and a runt-related transcription factor 2 (*Runx2*) gene, respectively.

Materials and Methods

Adenovirus Vectors

Ad vectors were constructed by an improved in vitro ligation method [20, 21]. The shuttle plasmids pHMCMV5, pHMCA5, and pHMEF5, which contain the cytomegalovirus (CMV) promoter, the CMV enhancer/β-actin promoter with β-actin intron (CA) promoter (a kind gift from Dr. J. Miyazaki, Osaka University, Osaka, Japan) [22], and the human elongation factor-1α (EF-1α) promoter, respectively, were constructed previously [16, 21]. The *mCherry* gene, which is derived from pmCherry (Clontech, Mountain View, CA, http://www.clontech.com), was inserted into pHMCMV5, pHMCA5, and pHMEF5, resulting in pHMCMV-mCherry, pHMCA-mCherry, and pHMEF-mCherry, respectively. pHMCMV-mCherry, pHMCA-mCherry, or pHMEF-mCherry was digested with I-*Ceu*I/PI-*Sce*I and ligated into I-*Ceu*I/PI-*Sce*I-digested pAdHM4 [20], resulting in pAd-CMV-mCherry, pAd-CA-mCherry, or pAd-EF-mCherry, respectively. Ad-CMV-mCherry, Ad-CA-mCherry, and Ad-EF-mCherry were generated and purified as described previously [17]. The Rous sarcoma virus (RSV) promoter-, the CMV promoter-, the CA promoter-, or the EF-1α promoter-driven β-galactosidase (LacZ)-expressing Ad vector (Ad-RSV-LacZ, Ad-CMV-LacZ, Ad-CA-LacZ, or Ad-EF-LacZ, respectively), the CA promoter-driven mouse PPARγ2-expressing Ad vector (Ad-CA-PPARγ2), the CA promoter-driven mouse Runx2-expressing Ad vector (Ad-CA-Runx2), and a transgene-deficient Ad vector (Ad-null), were generated previously [16, 17, 23, 24]. The vector particle (VP) titer and biological titer were determined by using a spectrophotometric method [25] and by means of an Adeno-X Rapid Titer Kit (Clontech), respectively. The ratios of the biological-to-particle titer were 1:31 for Ad-CMV-mCherry, 1:20 for Ad-CA-mCherry, 1:28 for Ad-EF-mCherry, 1:14 for Ad-CA-LacZ, 1:22 for Ad-EF-LacZ, 1:41 for Ad-RSV-LacZ, 1:21 for Ad-CMV-LacZ, 1:8 for Ad-CA-PPARγ2, 1:17 for Ad-CA-Runx2, and 1:11 for Ad-null.

Mouse ES and iPS Cell Cultures

Three mouse iPS cell clones 20D17, 38C2, and stm99-1 (a kind gift from Dr. S. Yamanaka, Kyoto University, Kyoto, Japan) were used in the present study (20D17 was purchased from Riken BioResource Center, Tsukuba, Japan, http://www.brc.riken.jp) [4, 26]. 20D17 and 38C2, both of which carry Nanog promoter-driven green fluorescent protein (GFP)/internal ribosomal entry site/puromycin-resistant gene, were generated from mouse embryonic fibroblasts (MEFs) [4], and stm99-1, carrying the Fbx15 promoter-driven β-geo cassette (a fusion of the β-galactosidase and neomycin resistance genes), was generated from gastric epithelial cells [26]. These mouse iPS cells and mouse E14 ES cells were routinely cultured in leukemia inhibitory factor-containing ES cell medium (Speciality Media) on mitomycin C-treated MEFs, and iPS cell lines and ES cells were passaged every 2nd day using 0.25% trypsin-EDTA (Invitrogen, Carlsbad, CA, http://www.invitrogen.com). Mouse iPS cells 20D17 and E14 ES cells were also cultured on a gelatin-coated dish. To obtain GFP-expressing undifferentiated cells, iPS cells 20D17 were cultured in ES cell medium containing 1.5 μg/ml puromycin (Sigma-Aldrich, St. Louis, MO, http://www.sigmaaldrich.com) on a gelatin-coated dish. Mouse iPS cell clone 20D17 was used in this report except where otherwise indicated. EB formation from mouse ES and iPS cells was induced using the hanging drop method as described previously [17].

LacZ Assay

Mouse ES cells or iPS cells (5×10^4 cells) were plated on 24-well plates. On the following day, they were transduced with each Ad vector (Ad-null, Ad-RSV-LacZ, Ad-CMV-LacZ, Ad-CA-LacZ, or Ad-EF-LacZ) at 3,000 VPs/cell for 1.5 hours. At 24 hours after incubation, X-galactosidase (Gal) staining was performed as described previously [16]. ES cell-derived EBs (ES-EBs) or iPS cell-derived EBs (iPS-EBs) cultured for 5 days (5d-ES-EBs or 5d-iPS-EBs, respectively) were transduced with each Ad vector at 3,000 VPs/cell. Two days later, LacZ expression was measured by X-Gal staining and β-Gal luminescence assays.

mCherry Expression Analysis

Mouse ES cells or iPS cells were plated on gelatin-coated 24-well plates. On the following day, they were transduced with the indicated dose of Ad-CA-mCherry or Ad-EF-mCherry for 1.5 hours. Twenty-four hours later, mCherry expression was analyzed by flow cytometry on an LSR II flow cytometer using FACSDiva software (BD Biosciences, Tokyo, Japan, http://www.bdbiosciences.com). To transduce the EB interior, the ES-EBs or iPS-EBs were transduced with 3,000 VPs/cell of Ad-CMV-mCherry or Ad-CA-mCherry three times on days 0, 2, and 5 (hereinafter referred to as triple transduction) [17]. In brief, 0d-ES-EBs or 0d-iPS-EBs (ES or iPS cell suspension, respectively) were transduced with Ad vector at 3,000 VPs/cell in a hanging drop for 2 days, and 2d-ES-EBs or 2d-iPS-EBs and 5d-ES-EBs or 5d-iPS-EBs were transduced with the same Ad vector at 3,000 VPs/cell for 1.5 hours. On day 7, mCherry expression in the ES-EBs or iPS-EBs was visualized via confocal microscopy (Leica TCS SP2 AOBS; Leica Microsystems, Tokyo, Japan, http://www.leica.com). The ES-EBs or iPS-EBs were then trypsinized and analyzed for mCherry expression by flow cytometry.

Expression of Coxsackievirus and Adenovirus Receptors

For detection of coxsackievirus and adenovirus receptor (CAR) expression, ES and iPS cells, both of which were cultured on gelatin-coated dishes, were harvested by using phosphate-buffered saline (PBS) containing 1 mM EDTA. Cells were then reacted

with rat anti-mouse CAR monoclonal antibody (kindly supplied from Dr. T. Imai, KAN Research Institute, Hyogo, Japan) and stained with phycoerythrin-labeled donkey anti-rat IgG (Jackson Immunoresearch Laboratories, West Grove, PA, http://www.jacksonimmuno.com). CAR expression was analyzed by using an LSR II flow cytometer.

In Vitro Differentiation

Two days after culture with a hanging drop, the EBs were transferred into a Petri dish and maintained for 3 days in suspension culture in differentiation medium (Dulbecco's modified Eagle's medium [Wako Chemical, Osaka, Japan, http://www.wako-chem.co.jp/english] supplemented with 15% fetal calf serum [Specialty Media, Inc., Phillipsburg, NJ, http://www.millipore.com], 0.1 mM 2-mercaptoethanol [Nacalai Tesque, Kyoto, Japan, http://www.nacalai.co.jp.en], 1× nonessential amino acid [Specialty Media, Inc.], 1× nucleosides [Specialty Media, Inc.], 2 mM L-glutamine [Invitrogen], and penicillin/streptomycin [Invitrogen]) containing 100 nM all-*trans*-retinoic acid (RA) (Wako Chemical) and then cultured for 2 more days in differentiation medium without RA [27, 28]. The cells were transduced with 3,000 VPs/cell of Ad vector (Ad-CA-LacZ, Ad-CA-PPARγ2, or Ad-CA-Runx2) at days 0, 2, and 5 as described above and plated on a gelatin-coated dish on day 7. For adipogenic or osteoblastic differentiation, cells were cultured in differentiation medium containing adipogenic supplements (0.1 M 3-isobutyl-L-methylxanthine [Sigma-Aldrich), 100 nM insulin [Sigma-Aldrich], 10 nM dexamethasone [Wako Chemical], and 2 nM triiodothyronine [Sigma-Aldrich]) or osteogenic supplements (50 μg/ml ascorbic acid 2-phosphate [Sigma-Aldrich]), 5 mM β-glycerophosphate [Sigma-Aldrich], and 10 nM dexamethasone [Wako Chemical]), respectively.

Biochemical Assays

Cells were cultured with adipogenic or osteogenic supplements for 15 days after plating on gelatin-coated plates. Adipocyte differentiation from mouse ES and iPS cells was evaluated by oil red O staining and glycerol-3-phosphate dehydrogenase (GPDH) activity. The oil red O staining and GPDH assay were performed using a Lipid Assay kit and GPDH Assay kit, respectively (Primary Cell Co., Ltd, Hokkaido, Japan, http://www.primarycell.com), according to the manufacturer's instructions. To detect matrix mineralization in the cells, cells were fixed with 4% paraformaldehyde-PBS and stained with $AgNO_3$ by the von Kossa method. To measure calcium deposition, cells were washed twice with PBS and decalcified with 0.5 M acetic acid, and cell culture plates were rotated overnight at room temperature. Insoluble material was removed by centrifugation. The supernatants were then assayed for calcium concentration with a calcium C-test kit (Wako Chemical). DNA in pellets was extracted using a DNeasy tissue kit (Qiagen, Valencia, CA, http://www1.qiagen.com), and calcium content was then normalized to cellular DNA. For the measurement of alkaline phosphatase (ALP) activity, cells were lysed in 10 mM Tris-HCl (pH 7.5) containing 1 mM $MgCl_2$ and 0.1% Triton X-100, and the lysates were then used for assay. ALP activity was measured using the LabAssay ALP kit (Wako Chemical) according to the manufacturer's instructions. The protein concentration of the lysates was determined using a Bio-Rad assay kit (Bio-Rad, Hercules, CA, http://www.bio-rad.com), and ALP activity was then normalized by protein concentration.

Reverse Transcription-Polymerase Chain Reaction

Total RNA was isolated from various kinds of cell populations with the use of ISOGENE (Nippon Gene, Tokyo, Japan, http://www.nippongene.com). cDNA was synthesized by using SuperScript II reverse transcriptase (RT) (Invitrogen) and the oligo(dT) primer. Polymerase chain reaction (PCR) was performed with the use of KOD Plus DNA polymerase (Toyobo, Osaka, Japan, http://www.toyobo.co.jp/e). The product was assessed by 2% agarose gel electrophoresis followed by ethidium bromide staining. The sequences of the primers used in this study are listed in supporting information Table S1.

Teratoma Formation and Histological Analysis

Mouse iPS cells were transduced with Ad-CA-mCherry at 10,000 VPs/cell for 1.5 hours. After culture for 3 days, mouse iPS cells were suspended at 1×10^7 cells/ml in PBS. Nude mice (8-10 weeks; Nippon SLC, Shizuoka, Japan, http://www.jslc.co.jp) were anesthetized with diethyl ether, and we injected 100 μl of the cell suspension (1×10^6 cells) subcutaneously into their backs. Five weeks later, tumors were surgically dissected from mice. Samples were washed, fixed in 10% formalin, and embedded in paraffin. After sectioning, the tissue was dewaxed in ethanol, rehydrated, and stained with hematoxylin and eosin. This process was commissioned to Applied Medical Research Laboratory (Osaka, Japan).

Results

Mouse iPS Cells Express Coxsackievirus and Adenovirus Receptor

In the present study, we mainly used the mouse iPS cell clone 20D17 [4]. To assess whether iPS cells have properties similar to those of ES cells under the present culture conditions, we initially investigated the expression of cellular marker genes of iPS cells (Fig. 1A). Semiquantitative RT-PCR analysis revealed that Oct-3/4 and Nanog, both of which are undifferentiated markers in ES cells, were strongly expressed in iPS cells. iPS cells also expressed GFP in the undifferentiated state only, because GFP expression was driven by the Nanog promoter [4]. By EB formation, the expression levels of Oct-3/4, Nanog, and GFP in iPS cells were decreased and, in turn, the three germ layer marker genes (ectoderm: nestin and fibroblast growth factor-5; mesoderm: brachyury T and flk-1; and endoderm: GATA-binding protein-6 and α-fetoprotein) were expressed. These results showed that the gene expression patterns of iPS cells were indistinguishable from those of ES cells.

We next examined the expression of CAR, a primary Ad receptor on the cellular surface, in iPS cells, because the expression of CAR is known to be essential for the transduction using the conventional Ad vector [29–31]. We have reported that CAR was highly expressed in mouse ES cells and ES-EBs [16, 17]. RT-PCR and flow cytometric analysis showed that CAR expression was observed in iPS cells and the expression level of CAR in iPS cells and iPS-EBs was equivalent to that in ES cells and ES-EBs, respectively (Fig. 1A, 1B). Notably, the expression of CAR was observed in more than 95% of GFP-expressing undifferentiated iPS cells. These results suggest that iPS cells could be efficiently transduced by using a conventional Ad vector.

Ad Vectors Containing the CA or the EF-1α Promoter Have Potent Transduction Activity in Mouse iPS Cells

To examine the transduction efficiency in iPS cells by using Ad vectors, we prepared LacZ-expressing Ad vectors under the control of four different promoters, the RSV promoter, the CMV promoter, the CA promoter, or the EF-1α promoter (Ad-RSV-LacZ, Ad-CMV-LacZ, Ad-CA-LacZ, or Ad-EF-LacZ, respectively). We also prepared Ad-null, a transgene-deficient Ad vector, as a control vector. ES and iPS cells were transduced with each Ad vector at 3,000 VPs/cell, and LacZ expression in the cells was measured. X-Gal staining showed that Ad-RSV-LacZ- or Ad-CMV-LacZ-transduced ES cells expressed little LacZ, whereas Ad-CA-LacZ- or Ad-EF-

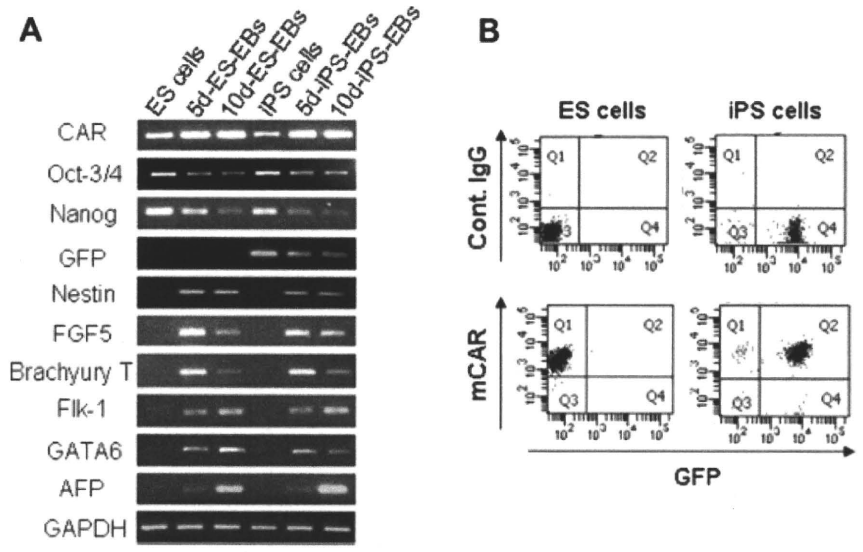

Figure 1. Gene expression patterns of mouse iPS cells were similar to those of mouse ES cells. **(A):** Total RNA was isolated from mouse ES cells (lane 1), 5d-ES-EBs (lane 2), 10d-ES-EBs (lane 3), iPS cells (lane 4), 5d-iPS-EBs (lane 5), or 10d-iPS-EBs (lane 6), and semiquantitative reverse transcriptase-polymerase chain reaction was then performed as described in Materials and Methods. The primers for Oct-3/4 and Nanog amplified both endogenous gene and exogenous factors. **(B):** The expression levels of CAR in mouse ES cells and iPS cells were detected with anti-mouse CAR monoclonal antibody by flow cytometry. As a negative control, the cells were incubated with an irrelevant antibody. Data shown are from one representative experiment of three performed. Abbreviations: AFP, α-fetoprotein; CAR, coxsackievirus and adenovirus receptor; Cont., control; EB, embryoid body; ES, embryonic stem; 5d-ES-EBs, ES cell-derived 5-day-cultured EBs; 10d-ES-EBs, ES cell-derived 10-day-cultured EBs; FGF, fibroblast growth factor; GAPDH, glyceraldehyde-3-phosphate dehydrogenase; GATA, GATA-binding protein; GFP, green fluorescent protein; iPS, induced pluripotent stem; 5d-iPS-EBs, iPS cell-derived 5-day-cultured EBs; 10d-iPS-EBs, iPS cell-derived 10-day-cultured EBs; mCAR, mouse CAR.

LacZ-transduced ES cells successfully expressed LacZ (Fig. 2A, top) as described previously [16]. Likewise, the CA and the EF-1α promoter but not the RSV or the CMV promoter exhibited potent transduction activity in iPS cells (Fig. 2A, bottom). Besides mouse iPS cell clone 20D17, mouse iPS cell clones 38C2 and stm99-1, which were generated from MEFs [4] and gastric epithelial cells [26], respectively, also efficiently expressed transgenes by an Ad vector containing the CA or EF-1α promoter (supporting information Fig. S1).

To confirm that the transgene was expressed in GFP-expressing undifferentiated iPS cells, we generated Ad-CA-mCherry and Ad-EF-mCherry, both of which express a monomeric DsRed variant, mCherry. Flow cytometric and fluorescent microscopic analysis showed that the mCherry expression was observed in GFP-expressing iPS cells transduced with Ad-CA-mCherry or Ad-EF-mCherry (Fig. 2B, supporting information Fig. S2). Furthermore, the expression of mCherry in iPS cells was dose-dependent, and more than 90% of the cells expressed mCherry after transduction with 10,000 VPs/cell of Ad-CA-mCherry and Ad-EF-mCherry (Fig. 2C and data not shown). Importantly, there was no significant difference in the percentage of GFP-positive cells between nontransduced cells and Ad-CA-mCherry- or Ad-EF-mCherry-transduced cells (Fig. 2D and data not shown). Moreover, neither alkaline phosphatase activity nor Oct-3/4 expression in iPS cells on day 3 after Ad vector-mediated transduction was different from that in nontransduced cells (supporting information Fig. 3). We also examined the pluripotency of Ad vector-transduced iPS cells by teratoma formation. Mouse iPS cells were transduced with Ad vector and were then injected subcutaneously into the backs of nude mice. After subcutaneous transplantation, we obtained teratomas containing epidermis, cartilage, and gut epithelial tissues (Fig. 2E). These observations demonstrated that the undifferentiated state and pluripotency in iPS cells were still maintained even after Ad vector transduction. Furthermore, we counted the number of viable iPS cells at 24, 48, and 72 hours after transduction to investigate the cytotoxicity in iPS cells transduced with Ad-CA-mCherry at 3,000 or 10,000 VPs/cell. The number of viable iPS cells transduced with Ad-CA-mCherry at 3,000 VPs/cell was comparable to the number of viable nontransduced iPS cells, whereas the number of viable iPS cells was slightly (but not significantly) reduced in Ad-CA-mCherry-transduced iPS cells at 10,000 VPs/cell (Fig. 2F). This result was quite similar to that for ES cells (Fig. 2F), and our data suggest that Ad vector transduction has almost no cytotoxicity against either mouse ES cells or mouse iPS cells. These results clearly demonstrated that an Ad vector containing the CA or the EF-1α promoter is an appropriate vector for both ES cells and iPS cells and that iPS cells have the same features as ES cells in terms of Ad vector-mediated transduction.

Ad Vectors Containing the CA Promoter Robustly Drove Transgene Expression in iPS-EBs

We next performed a transduction experiment for ES-EBs and iPS-EBs using a LacZ-expressing Ad vector. Consistent with our previous report [17], the CA promoter showed the highest LacZ expression in ES-EBs. Similarly, the CA promoter showed the highest transduction efficiency in iPS-EBs (Fig. 3A, 3B). Interestingly, the CMV promoter had strong activity in iPS-EBs despite its weak activity in ES cells, ES-EBs, and undifferentiated iPS cells (Figs. 2A, 3A, 3B). These phenomena were also observed by using other iPS cell clone-derived EBs (supporting information Fig. 4).

We next attempted to express the transgene inside the ES-EBs and iPS-EBs, as it is considered to be essential to express the transgene in the EB interior to differentiate ES cells or iPS cells into functional cells. Thus, ES-EBs and iPS-EBs were transduced in triplicate with Ad-CMV-mCherry or Ad-CA-mCherry. This transduction method, namely the triple transduction method, is a gene transfer method that uses an Ad vector to express the transgene in the EB interior (see

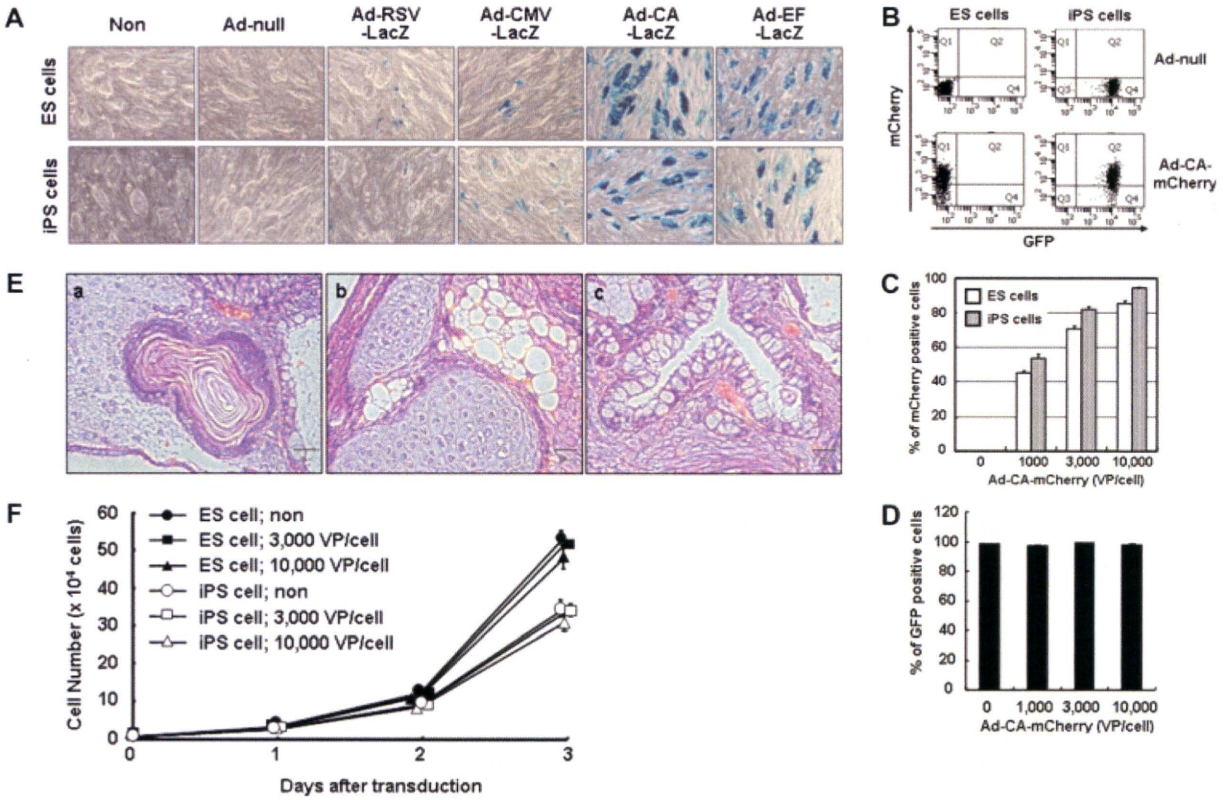

Figure 2. Efficient transgene expression in mouse iPS cells by using an Ad vector containing the CA and the EF-1α promoter. **(A):** Mouse ES cells or iPS cells were transduced with a LacZ-expressing Ad vector at 3,000 VPs/cell. On the following day, X-galactosidase (Gal) staining was carried out. Similar results for X-Gal staining were obtained in three independent experiments. **(B):** Mouse ES cells or iPS cells were transduced with Ad-CA-mCherry at 3,000 VPs/cell, and mCherry-expressing cells were then analyzed by flow cytometry. **(C, D):** Mouse ES cells or iPS cells were transduced with different amounts of Ad-CA-mCherry for 1.5 hours. mCherry expression **(C)** and GFP expression **(D)** were determined by flow cytometry. The data are expressed as the mean ± SD ($n = 3$). **(E):** Paraffin sections of the teratomas derived from Ad-CA-mCherry-transduced iPS cells were prepared, and sections were stained with hematoxylin and eosin: a, ectoderm (epidermis); b, mesoderm (cartilage and adipocyte); c, endoderm (gut epithelium) **(F):** After adenoviral transduction, viable mouse ES cells or iPS cells were counted. Data are expressed as the mean ± SD ($n = 3$). Abbreviations: Ad, adenovirus; CA, cytomegalovirus enhancer/β-actin promoter; CMV, cytomegalovirus; EF, elongation factor-1α; ES, embryonic stem; GFP, green fluorescent protein; IPS, induced pluripotent stem; LacZ, β-galactosidase; RSV, Rous sarcoma virus; VP, vector particle.

Materials and Methods) [17]. Confocal microscopic analysis revealed mCherry expression interior in ES-EBs or iPS-EBs by triple transduction, whereas mCherry expression was observed only in the periphery of the ES-EBs or iPS-EBs by single transduction (Fig. 3C). The percentage of mCherry-positive cells in the ES-EBs or iPS-EBs transduced in triplicate with Ad-CA-mCherry was 43% or 56%, respectively, as determined by flow cytometry (Fig. 3C). In addition, confocal microscopic analysis and flow cytometric analysis showed that Ad-CMV-mCherry-transduced ES-EBs expressed little mCherry even using the triple transduction method, whereas iPS-EBs transduced in triplicate with Ad-CMV-mCherry expressed mCherry only in the periphery of the iPS-EBs. These results are in agreement with LacZ expression in Ad-CMV-LacZ-transduced iPS-EBs as described above. Our data demonstrated that, as in the case of ES cells and ES-EBs, the choice of a suitable promoter was important for efficient transduction in iPS cells and iPS-EBs.

Adipocyte and Osteoblast Differentiation of Mouse iPS Cells Was Facilitated by Ad Vector Transduction

We have shown previously that adipocyte differentiation from mouse ES cells is enhanced by the transduction of the *PPARγ* gene, which is known to be a master regulator gene for adipogenesis [18, 19], into ES cells and ES-EBs using an Ad vector. In this study, to examine whether adipocyte differentiation from iPS cells could also be promoted by Ad vector-mediated transduction and to compare the adipogenic potential between ES cells and iPS cells, both types of cells were differentiated into adipocytes by the transduction of the *PPARγ* gene using the triple transduction method described above. Oil red O staining after culturing for 15 days revealed that lipid droplets were accumulated in both ES cell-derived cells and iPS cell-derived cells by culturing with adipogenic supplements, although the level of lipid accumulation in iPS cell-derived cells was lower than that in ES cells-derived cells (Fig. 4A). In the presence of adipogenic supplements, the percentage of oil red O-positive cells in nontransduced or Ad-CA-LacZ-transduced ES-EBs was approximately 50%, whereas 20%-30% of the nontransduced or Ad-CA-LacZ-transduced iPS-EBs were positive for oil red O. Importantly, adipocyte differentiation in Ad-CA-PPARγ-transduced cells was more efficient than that in nontransduced or Ad-CA-LacZ-transduced cells (Fig. 4A). Oil red O-positive cells in Ad-CA-PPARγ-transduced ES cell- or iPS cell-derived cells were more than 90% or 80% of the total cells, respectively. Furthermore, enhanced adipocyte differentiation from PPARγ-transduced ES and iPS cells was also confirmed by measuring the activity of GPDH and the expression of marker genes

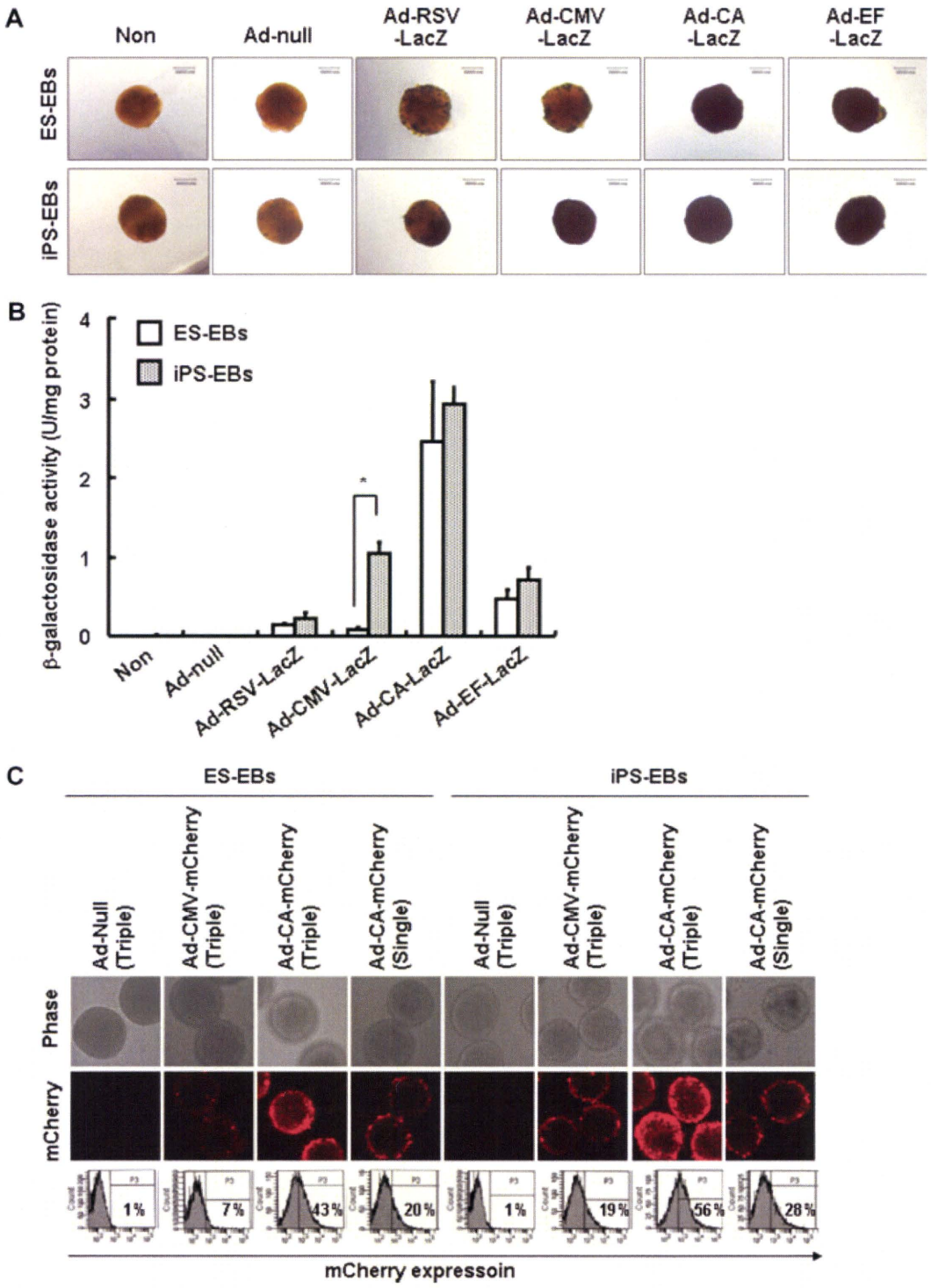

Figure 3. Comparison of promoter activity in iPS-EBs by using Ad vectors. ES cell-derived or IPS cell-derived 5-day-cultured EBs were transduced with each Ad vector at 3,000 vector particles/cell. After 48 hours, X-galactosidase (Gal) staining **(A)** and a β-galactosidase luminescence assay **(B)** were performed as described in Materials and Methods. **(A):** Similar results of X-gal staining were obtained in six independent experiments. **(B):** Data are expressed as the mean $\pm$ SD ($n = 3$). *, $p < .01$ **(C):** Either ES-EBs or iPS-EBs was transduced with Ad vectors by triple transduction (Triple) or by single transduction (Single). mCherry expression in ES-EBs or iPS-EBs was detected by confocal microscopy and flow cytometry. As a negative control, both types of EBs were transduced with Ad-null by triple transduction. Abbreviations: Ad, adenovirus; CA, cytomegalovirus enhancer/β-actin promoter; CMV, cytomegalovirus; EB, erythroid body; EF, elongation factor-1α; ES, embryonic stem; IPS, induced pluripotent stem; LacZ, β-galactosidase; RSV, Rous sarcoma virus.

characteristic of adipocyte differentiation (Fig. 4B, 4C). Interestingly, iPS cells were more efficiently differentiated into adipocytes than were ES cells after Ad vector transduction. The GPDH activity in PPARγ-transduced ES cells was twofold higher than that in nontransduced or LacZ-transduced ES cells, whereas PPARγ-transduced iPS cells showed

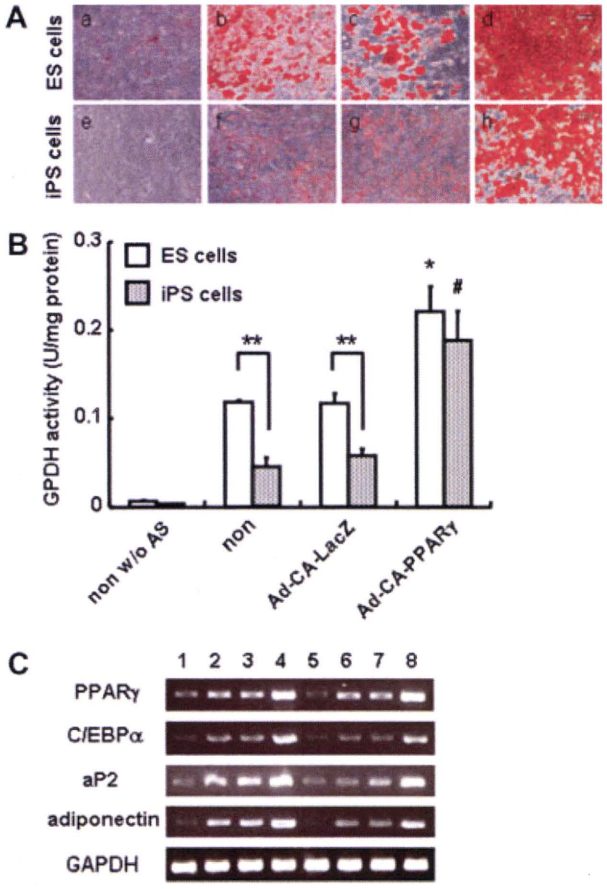

Figure 4. Efficient adipocyte differentiation from mouse ES cells and iPS cells by the transduction of the *PPARγ* gene. ES-EBs or iPS-EBs were transduced in triplicate with 10,000 vector particles/cell of Ad-CA-LacZ or Ad-CA-PPARγ. After plating onto a gelatin-coated dish on day 7, ES-EBs and iPS-EBs were cultured for 15 days in the presence or absence of AS. After cultivation, **(A)** lipid accumulation was detected by oil red O staining, and **(B)** GPDH activity in the cells was measured. **(A):** a, nontreated ES-EBs; b, ES-EBs with AS; c, ES-EBs with AS plus Ad-CA-LacZ; d, ES-EBs with AS plus Ad-CA-PPARγ; e, nontreated iPS-EBs; f, iPS-EBs with AS; g, iPS-EBs with AS plus Ad-CA-LacZ; h, iPS-EBs with AS plus Ad-CA-PPARγ. Scale bar = 60 μm. **(B):** Data are expressed as the mean ± SD (n = 3). *, $p < .01$; **, $p < .05$, compared with nontransduced or Ad-CA-LacZ-transduced ES cells. #, $p < .05$, compared with nontransduced or Ad-CA-LacZ-transduced iPS cells. **(C):** Expression of PPARγ, C/EBPα, aP2, adiponectin, and GAPDH was measured by semiquantitative reverse transcriptase-polymerase chain reaction. Lane 1, nontreated ES-EBs; lane 2, ES-EBs with AS; lane 3, ES-EBs with AS plus Ad-CA-LacZ; lane 4, ES-EBs with AS plus Ad-CA-PPARγ; lane 5, nontreated iPS-EBs; lane 6, iPS-EBs with AS; lane 7, iPS-EBs with AS plus Ad-CA-LacZ; lane 8, iPS-EBs with AS plus Ad-CA-PPARγ. Abbreviations: AD, adenovirus; AS, adipogenic supplements; CA, cytomegalovirus enhancer/β-actin promoter; C/EBPα, CCAAT/enhancer binding protein α; ES, embryonic stem; EB, erythroid body; GAPDH, glyceraldehyde-3-phosphate dehydrogenase; GPDH, glycerol-3-phosphate dehydrogenase; IPS, induced pluripotent stem; LacZ, β-galactosidase; PPARγ, peroxisome proliferator-activated receptor γ; w/o, without.

approximately fourfold higher GPDH activity than nontransduced or LacZ-transduced iPS cells. These results showed that, like ES cells, iPS cells could be differentiated into adipocytes and that this adipocyte differentiation could be markedly facilitated by transient *PPARγ* gene transduction using an Ad vector.

Because Ad vector-mediated functional gene transduction was found to be effective to increase the differentiation efficiency from ES and iPS cells, we expected that other functional cells could be efficiently differentiated from ES and iPS cells by using an Ad vector. To confirm this finding, both types of cells were differentiated into osteoblasts by Ad vector-mediated transduction of a *Runx2* gene, which was previously proven to be indispensable for osteoblast differentiation [32, 33]. ES and iPS cells were transduced in triplicate with Ad-CA-LacZ or Ad-CA-Runx2 and were cultured with osteogenic supplements. We initially examined activity of ALP, an early osteoblast differentiation marker, in both types of cells, and showed that Ad-CA-Runx2-transduced cells exhibited higher ALP activity than nontransduced or Ad-CA-LacZ-transduced cells (Fig. 5A). These results indicated that early osteoblast differentiation was promoted by Ad vector-mediated *Runx2* gene transfer. Next, to estimate the mature osteoblast differentiation, matrix mineralization in the cells was detected by von Kossa staining. Consistent with the previous report [34], treatment with osteogenic supplements resulted in matrix mineralization in both types of cells, whereas in the absence of additives no calcification was observed (Fig. 5B). We also found that osteoblast differentiation from both ES and iPS cells could be dramatically promoted by Ad vector-mediated *Runx2* gene transduction (Fig. 5B). The level of calcium in Ad-CA-Runx2-transduced ES or iPS cells was approximately eightfold higher than that of nontransduced or Ad-CA-LacZ-transduced cells (Fig. 5C). Semiquantitative RT-PCR analysis also showed that the expression levels of Runx2, osterix, bone sialoprotein, osteocalcin, and type I collagen mRNA were up-regulated in the cells transduced with Ad-CA-Runx2 (Fig. 5D). These results demonstrated that the osteogenic potential in iPS cells was equal to that in ES cells and that efficient osteoblast differentiation from ES and iPS cells could be achieved by exogenous Runx2 expression using optimized Ad vectors.

Discussion

The establishment of an efficient gene transfer system for pluripotent cells would be quite useful for the application of these cells to regenerative medicine. We have previously developed suitable Ad vectors for transducing an exogenous gene into mouse ES cells and ES-EBs and showed that these Ad vectors could be successfully applied to regenerative medicine and basic studies [16, 17]. The aim of this study was to characterize the efficiency of transduction with Ad vectors in mouse iPS cells and to develop efficient methods for inducing the differentiation of mouse iPS cells by means of Ad vector transduction. This is the first study to report the detailed transduction properties of various types of Ad vectors in mouse iPS cells.

We optimized the transduction activity in mouse iPS cells and iPS-EBs by comparing four types of promoters (RSV, CMV, CA, and EF-1α) using Ad vectors. Because iPS cells have been shown to possess mostly the same properties as ES cells [4–6] and the CA and the EF-1α promoter exhibited strong transduction activity in mouse ES cells [16], we speculated that the same results might be obtained in mouse iPS cells. As we expected, mouse iPS cells and iPS-EBs were capable of being efficiently transduced by using a conventional Ad vector containing the CA (and the EF-1α) promoter (Figs. 2A, 3, supporting information Figs. S1, S2, S4). We found that a primary Ad receptor, CAR, was highly expressed in iPS cells (Fig. 1), which were generated from MEFs [4],

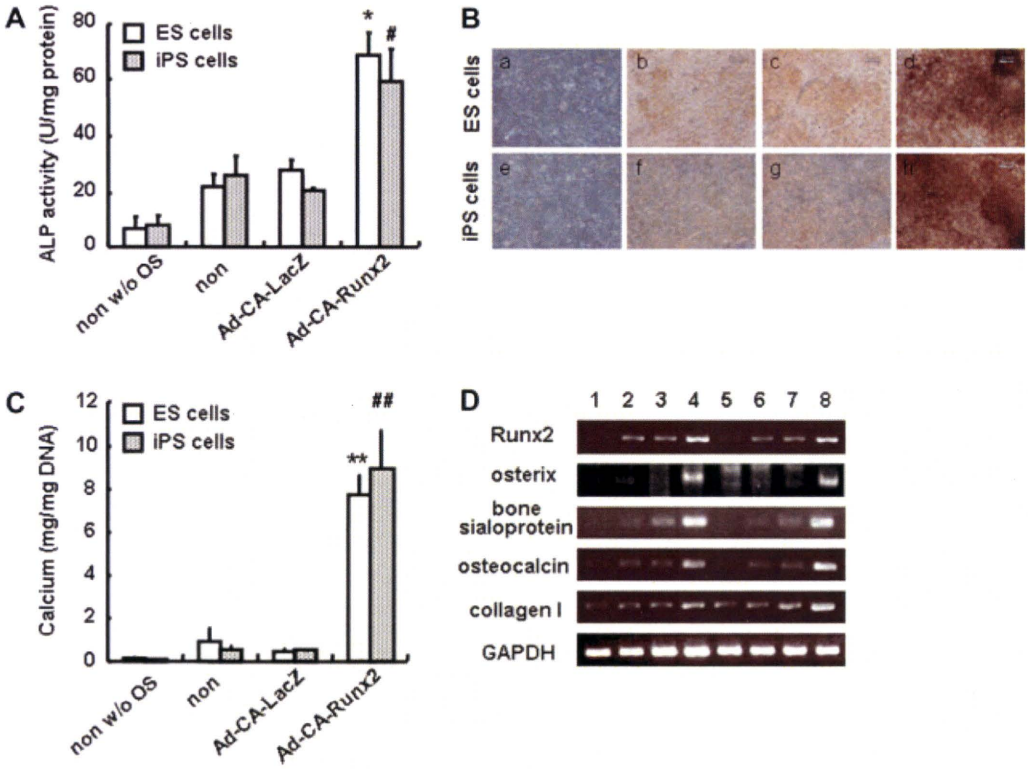

Figure 5. Enhanced osteoblast differentiation from ES cells and iPS cells in Ad-CA-Runx2-transduced cells. **(A):** ES-EBs or iPS-EBs were transduced in triplicate with 10,000 vector particles/cell of Ad-CA-LacZ or Ad-CA-Runx2. After culturing for 15 days with or without OS, ALP activity in the cells was determined. Data are expressed as the mean ± SD ($n = 3$). *, $p < .05$, compared with nontransduced or Ad-CA-LacZ-transduced ES cells. #, $p < .05$, compared with nontransduced or Ad-CA-LacZ-transduced iPS cells. Matrix mineralization in the cells was detected by von Kossa staining **(B)** and deposition of calcium was quantified as described in Materials and Methods **(C)**. **(B):** a, nontreated ES-EBs; b, ES-EBs with OS; c, ES-EBs with OS plus Ad-CA-LacZ; d, ES-EBs with OS plus Ad-CA-Runx2; e, nontreated iPS-EBs; f, iPS-EBs with OS; g, iPS-EBs with OS plus Ad-CA-LacZ; h, iPS-EBs with OS plus Ad-CA-Runx2. Scale bar = 60 μm. **(C):** Data are expressed as the mean ± SD ($n = 3$). **, $p < .01$, compared with nontransduced or Ad-CA-LacZ-transduced cells. ##, $p < .01$, compared with nontransduced or Ad-CA-LacZ-transduced iPS cells. **(D):** Total RNA was isolated, and semiquantitative reverse transcriptase-polymerase chain reaction was performed using primers for Runx2, osterix, bone sialoprotein, osteocalcin, collagen type I, and GAPDH. Lane 1, nontreated ES-EBs; lane 2, ES-EBs with OS; lane 3, ES-EBs with OS plus Ad-CA-LacZ; lane 4, ES-EBs with OS plus Ad-CA-Runx2; lane 5, nontreated iPS-EBs; lane 6, iPS-EBs with OS; lane 7, iPS-EBs with OS plus Ad-CA-LacZ; lane 8, iPS-EBs with OS plus Ad-CA-Runx2. Abbreviations: AD, adenovirus; ALP, alkaline phosphatase; CA, cytomegalovirus enhancer/β-actin promoter; ES, embryonic stem; EB, erythroid body; GAPDH, glyceraldehyde-3-phosphate dehydrogenase; IPS, induced pluripotent stem; LacZ, β-galactosidase; OS, osteogenic supplements; Runx2, runt-related transcription factor 2; w/o, without.

despite the low levels of CAR expression in MEFs [16]. This would lead to high transduction efficiency in mouse iPS cells when conventional Ad vectors containing the CA and the EF-1α promoter were used. In addition, we showed that more than 80% or 90% of the mouse iPS cells expressed mCherry after transduction with the Ad vector containing the CA promoter at 3,000 or 10,000 VPs/cell, respectively, without any decrease in the expression of pluripotent genes or viability (Fig. 2B–2D, 2F, supporting information Figs. 2, 3). Notably, Ad vector-transduced iPS cells still exhibited teratoma formation in vivo (Fig. 2E), and the efficiency of adipocyte or osteoblast differentiation in Ad-CA-LacZ-transduced iPS cells was similar to that in nontransduced iPS cells (Figs. 4, 5), indicating that Ad vector transduction did not change the pluripotency of iPS cells. These results indicate that gene transfer into mouse ES and iPS cells using an optimized conventional Ad vector would be useful for the application of these cells to both regenerative medicine and basic research.

We found that the CMV promoter, which is currently in wide use in transduction experiments, had weak activity in both mouse ES cells [16, 35] and mouse iPS cells (Fig. 2A, supporting information Fig. S1). Several groups have reported that undifferentiated ES cells expressed low levels of transgene when the CMV promoter was used, whereas the expression levels of reporter genes, when driven by the CMV promoter, were markedly increased in ES cell-derived neurons or cardiomyocytes [36, 37]. Consistent with our results (Fig. 3, supporting information Fig. S4), other authors have shown that the activity of the CMV promoter in ES-EBs was also lower than that of the CA and the EF-1α promoters [37]. These results suggest that the CMV promoter in the Ad vector would be silenced, possibly owing to DNA methylation [38] in mouse ES, ES-EB, and iPS cells. Interestingly, we observed that the CMV promoter was more strongly activated in mouse iPS-EBs than in ES-EBs (Fig. 3, supporting information Fig. S4). We have no idea why the CMV promoter was able to drive robust transgene expression in mouse iPS-EBs. It is possible that cellular types that comprise iPS-EBs might be different from those of ES-EBs because iPS cells showed slightly slower proliferation than ES cells (Fig. 2F) [4], which may have led to the difference in the transduction efficiency in iPS-EBs and ES-EBs when the CMV promoter was used. On the other hand, the expression levels of the three germ layer marker genes in iPS-EBs were largely comparable to those in ES-EBs (Fig. 1A), suggesting that, as for ES cells, iPS cells differentiate into ectoderm, mesoderm, and endoderm cells. Therefore, which kinds of cells in iPS-EBs

could express transgenes after the transduction with Ad vector containing the CMV promoter should be investigated. As with iPS-EBs, it has been reported that human ES cells and human ES cell-derived EBs, albeit not all ES cell clones, could also be transduced with an Ad vector containing the CMV promoter [39, 40]. Hence, further analysis of the precise mechanism regulating the CMV promoter in stem cells will be also needed.

We observed that mouse iPS cells could be differentiated into adipocytes and osteoblasts using the same protocols as those used for mouse ES cells (Figs. 4, 5). However, mouse iPS cells showed less efficient adipocyte differentiation than ES cells (Fig. 4), although almost no difference in osteoblast differentiation was observed between ES and iPS cells. *aP2* is a valuable indicator of adipocyte differentiation but there is no evidence that *aP2* is an adipocyte master gene (Fig. 4C). In addition, mouse iPS cells proliferated more slowly than ES cells as described above (Fig. 2F) [4], and thus their differentiation into adipocytes may have been delayed. To examine whether this is a general difference between ES and iPS cells or a specific characteristic of 20D17, we attempted to differentiate other iPS cell clones (38C2 and stm99-1) into adipocytes. Oil red O staining showed that the efficiency of adipocyte differentiation in 38C2-derived cells was equivalent to that in ES cell-derived cells, whereas stm99-1, like 20D17, had slightly less adipogenic potential than ES cells (supporting information Fig. S5). This result suggests that there is a difference in the differentiation potential among iPS cell clones. Therefore, to differentiate iPS cells into functional cells, the choice of appropriate iPS cell clone would be essential.

We showed that the efficiency of adipocyte differentiation from iPS cells was significantly increased by the triple transduction of the *PPARγ* gene (Fig. 4). We found previously that single transduction with Ad-CA-PPARγ into ES-EBs at day 5 was not enough for enhancing the adipocyte differentiation (our unpublished data). Although the transgene was not expressed in all of the cells that comprise ES-EBs or iPS-EBs even by triple transduction (Fig. 3C), transgene expression by at least triple transduction, but not by single transduction, should be necessary to trigger efficient differentiation. Thus, we concluded that gene transduction in triplicate into iPS cells would be required for promoting the differentiation of iPS cells into functional cells. Notably, PPARγ transduction in mouse iPS cells was more effective than that in mouse ES cells probably because the efficiency of Ad vector transduction was higher in mouse iPS cells than in mouse ES cells (Fig. 2C). Our data thus demonstrate that our transduction system can be successfully applied to mouse iPS cells. We also succeeded in efficient osteoblast differentiation from mouse ES cells and iPS cells by Ad vector-mediated Runx2 transduction. Previously, Tai et al. [41] reported that stable transduction of the *osterix* gene, which is required for osteoblastogenesis [42], in mouse ES cells promoted osteoblast differentiation. However, a *Runx2* gene transfer into either ES cells or iPS cells is considered to be more appropriate for differentiation into osteoblasts than an *osterix* gene, because Runx2 is necessary for mesenchymal cell differentiation toward mature osteoblasts [43] and osterix has been shown to function downstream of Runx2 [42]. Indeed, the expression levels of osterix mRNA were increased in Runx2-transduced cells (Fig. 5D). Furthermore, constitutive transgene expression might lead to undesirable effects, such as oncogenesis, after cellular differentiation. Therefore, we conclude that transient transduction of the *Runx2* gene into ES and iPS cells is preferable for efficient differentiation into osteoblasts and that our system could be a powerful tool to promote the cellular differentiation of mouse ES and iPS cells.

In summary, we developed an efficient gene delivery system for mouse iPS cells and demonstrated that this system is effective in promoting cellular differentiation. As for ES cells, mouse iPS cells could be differentiated into not only adipocytes and osteoblasts but also cardiomyocytes [44], cardiovascular cells [45], and hematopoietic cells [46], and iPS cells thus would be an ideal source of cells for regenerative medicine. More recently, it was demonstrated that mouse iPS cells could be generated by transduction of reprogrammed factors using Ad vectors [47] or nonviral vectors [48] and that the reprogrammed factors were not integrated in their genomes. Because these nonintegrated iPS cells also have the same characteristics as ES cells and reprogrammed factor-integrated iPS cells, our system would probably be applicable for nonintegrated iPS cells. Therefore, our transient expression system using Ad vectors could be a valuable tool for application to safer regenerative medicine using iPS cells.

Acknowledgments

We thank Dr. S. Yamanaka for kindly providing the mouse iPS cell lines 20D17, 38C2, and stm99-1. We also thank Dr. J. Miyazaki and Dr. T. Imai for providing the CA promoter and anti-mouse CAR monoclonal antibody, respectively. This work was supported by grants from the Ministry of Health, Labor, and Welfare of Japan. K.T. is a Research Fellow of the Japan Society for the Promotion of Science.

Disclosure of Potential Conflicts of Interest

The authors indicate no potential conflicts of interest.

References

1 Evans MJ, Kaufman MH. Establishment in culture of pluripotential cells from mouse embryos. Nature 1981;292:154–156.
2 Thomson JA, Itskovitz-Eldor J, Shapiro SS et al. Embryonic stem cell lines derived from human blastocysts. Science 1998;282: 1145–1147.
3 Takahashi K, Yamanaka S. Induction of pluripotent stem cells from mouse embryonic and adult fibroblast cultures by defined factors. Cell 2006;126:663–676.
4 Okita K, Ichisaka T, Yamanaka S. Generation of germline-competent induced pluripotent stem cells. Nature 2007;448:313–317.
5 Maherali N, Sridharan R, Xie W et al. Directly reprogrammed fibroblasts show global epigenetic remodeling and widespread tissue contribution. Cell Stem Cell 2007;1:55–70.
6 Wernig M, Meissner A, Foreman R et al. In vitro reprogramming of fibroblasts into a pluripotent ES-cell-like state. Nature 2007;448: 318–324.
7 Takahashi K, Tanabe K, Ohnuki M et al. Induction of pluripotent stem cells from adult human fibroblasts by defined factors. Cell 2007; 131:861–872.
8 Yu J, Vodyanik MA, Smuga-Otto K et al. Induced pluripotent stem cell lines derived from human somatic cells. Science 2007;318: 1917–1920.
9 Lowry WE, Richter L, Yachechko R et al. Generation of human induced pluripotent stem cells from dermal fibroblasts. Proc Natl Acad Sci UlSlA 2008;105:2883–2888.
10 Park IH, Zhao R, West JA et al. Reprogramming of human somatic cells to pluripotency with defined factors. Nature 2008;451:141–146.
11 Kyba M, Perlingeiro RC, Daley GQ. HoxB4 confers definitive lymphoid-myeloid engraftment potential on embryonic stem cell and yolk sac hematopoietic progenitors. Cell 2002;109:29–37.

12 Liew CG, Shah NN, Briston SJ et al. PAX4 enhances β-cell differentiation of human embryonic stem cells. PLoS ONE 2008;3:e1783.
13 Chung S, Sonntag KC, Andersson T et al. Genetic engineering of mouse embryonic stem cells by Nurr1 enhances differentiation and maturation into dopaminergic neurons. Eur J Neurosci 2002;16: 1829–1838.
14 Kovesdi I, Brough DE, Bruder JT et al. Adenoviral vectors for gene transfer. Curr Opin Biotechnol 1997;8:583–589.
15 Benihoud K, Yeh P, Perricaudet M. Adenovirus vectors for gene delivery. Curr Opin Biotechnol 1999;10:440–447.
16 Kawabata K, Sakurai F, Yamaguchi T et al. Efficient gene transfer into mouse embryonic stem cells with adenovirus vectors. Mol Ther 2005;12:547–554.
17 Tashiro K, Kawabata K, Sakurai H et al. Efficient adenovirus vector-mediated PPAR gamma gene transfer into mouse embryoid bodies promotes adipocyte differentiation. J Gene Med 2008;10:498–507.
18 Tontonoz P, Hu E, Spiegelman BM. Stimulation of adipogenesis in fibroblasts by PPARγ2, a lipid-activated transcription factor. Cell 1994;79:1147–1156.
19 Rosen ED, Sarraf P, Troy AE et al. PPARγ is required for the differentiation of adipose tissue in vivo and in vitro. Mol Cell 1999;4: 611–617.
20 Mizuguchi H, Kay MA. Efficient construction of a recombinant adenovirus vector by an improved in vitro ligation method. Hum Gene Ther 1998;9:2577–2583.
21 Mizuguchi H, Kay MA. A simple method for constructing E1- and E1/E4-deleted recombinant adenoviral vectors. Hum Gene Ther 1999; 10:2013–2017.
22 Niwa H, Yamamura K, Miyazaki J. Efficient selection for high-expression transfectants with a novel eukaryotic vector. Gene 1991; 108:193–199.
23 Sakurai H, Tashiro K, Kawabata K et al. Adenoviral expression of suppressor of cytokine signaling-1 reduces adenovirus vector-induced innate immune responses. J Immunol 2008;180:4931–4938.
24 Tashiro K, Kondo A, Kawabata K et al. Efficient osteoblast differentiation from mouse bone marrow stromal cells with polylysin-modified adenovirus vectors. Biochem Biophys Res Commun 2009;379: 127–132.
25 Maizel JV Jr, White DO, Scharff MD. The polypeptides of adenovirus. I. Evidence for multiple protein components in the virion and a comparison of types 2, 7A, and 12. Virology 1968;36:115–125.
26 Aoi T, Yae K, Nakagawa M et al. Generation of pluripotent stem cells from adult mouse liver and stomach cells. Science 2008;321:699–702.
27 Dani C, Smith AG, Dessolin S et al. Differentiation of embryonic stem cells into adipocytes in vitro. J Cell Sci 1997;110(Pt 11): 1279–1285.
28 Kawaguchi J, Mee PJ, Smith AG. Osteogenic and chondrogenic differentiation of embryonic stem cells in response to specific growth factors. Bone 2005;36:758–769.
29 Bergelson JM, Cunningham JA, Droguett G et al. Isolation of a common receptor for Coxsackie B viruses and adenoviruses 2 and 5. Science 1997;275:1320–1323.
30 Tomko RP, Xu R, Philipson L. HCAR and MCAR: the human and mouse cellular receptors for subgroup C adenoviruses and group B coxsackieviruses. Proc Natl Acad Sci UlSlA 1997;94:3352–3356.
31 Mizuguchi H, Hayakawa T. Targeted adenovirus vectors. Hum Gene Ther 2004;15:1034–1044.
32 Ducy P, Zhang R, Geoffroy V et al. Osf2/Cbfa1: a transcriptional activator of osteoblast differentiation. Cell 1997;89:747–754.
33 Komori T, Yagi H, Nomura S et al. Targeted disruption of Cbfa1 results in a complete lack of bone formation owing to maturational arrest of osteoblasts. Cell 1997;89:755–764.
34 zur Nieden NI, Kempka G, Ahr HJ. In vitro differentiation of embryonic stem cells into mineralized osteoblasts. Differentiation 2003;71: 18–27.
35 Chung S, Andersson T, Sonntag KC et al. Analysis of different promoter systems for efficient transgene expression in mouse embryonic stem cell lines. Stem Cells 2002;20:139–145.
36 Rust EM, Westfall MV, Samuelson LC et al. Gene transfer into mouse embryonic stem cell-derived cardiac myocytes mediated by recombinant adenovirus. In Vitro Cell Dev Biol Anim 1997;33:270–276.
37 Hong S, Hwang DY, Yoon S et al. Functional analysis of various promoters in lentiviral vectors at different stages of in vitro differentiation of mouse embryonic stem cells. Mol Ther 2007;15: 1630–1639.
38 Brooks AR, Harkins RN, Wang P et al. Transcriptional silencing is associated with extensive methylation of the CMV promoter following adenoviral gene delivery to muscle. J Gene Med 2004;6: 395–404.
39 Rufaihah AJ, Haider HK, Heng BC et al. Directing endothelial differentiation of human embryonic stem cells via transduction with an adenoviral vector expressing the VEGF(165) gene. J Gene Med 2007; 9:452–461.
40 Brokhman I, Pomp O, Shaham L et al. Genetic modification of human embryonic stem cells with adenoviral vectors: differences of infectability between lines and correlation of infectability with expression of the coxsackie and adenovirus receptor. Stem Cells Dev 2009;18: 447–456.
41 Tai G, Polak JM, Bishop AE et al. Differentiation of osteoblasts from murine embryonic stem cells by overexpression of the transcriptional factor osterix. Tissue Eng 2004;10:1456–1466.
42 Nakashima K, Zhou X, Kunkel G et al. The novel zinc finger-containing transcription factor osterix is required for osteoblast differentiation and bone formation. Cell 2002;108:17–29.
43 Marie PJ. Transcription factors controlling osteoblastogenesis. Arch Biochem Biophys 2008;473:98–105.
44 Mauritz C, Schwanke K, Reppel M et al. Generation of functional murine cardiac myocytes from induced pluripotent stem cells. Circulation 2008;118:507–517.
45 Narazaki G, Uosaki H, Teranishi M et al. Directed and systematic differentiation of cardiovascular cells from mouse induced pluripotent stem cells. Circulation 2008;118:498–506.
46 Schenke-Layland K, Rhodes KE, Angelis E et al. Reprogrammed mouse fibroblasts differentiate into cells of the cardiovascular and hematopoietic lineages. Stem Cells 2008;26:1537–1546.
47 Stadtfeld M, Nagaya M, Utikal J et al. Induced pluripotent stem cells generated without viral integration. Science 2008;322:945–949.
48 Okita K, Nakagawa M, Hyenjong H et al. Generation of mouse induced pluripotent stem cells without viral vectors. Science 2008; 322:949–953.

See www.StemCells.com for supporting information available online.

HUMAN GENE THERAPY 21:1273–1285 (October 2010)

DOI: 10.1089/hum.2009.223

Characterization of a Recombinant Adeno-Associated Virus Type 2 Reference Standard Material

Martin Lock,[1] Susan McGorray,[2] Alberto Auricchio,[3,4] Eduard Ayuso,[5] E. Jeffrey Beecham,[6] Véronique Blouin-Tavel,[7] Fatima Bosch,[5] Mahuya Bose,[8] Barry J. Byrne,[9,10] Tina Caton,[8] John A. Chiorini,[11] Abdelwahed Chtarto,[12,13] K. Reed Clark,[14,15] Thomas Conlon,[10] Christophe Darmon,[7] Monica Doria,[4] Anne Douar,[16] Terence R. Flotte,[17,18] Joyce D. Francis,[8] Achille Francois,[7] Mauro Giacca,[19] Michael T. Korn,[1] Irina Korytov,[10] Xavier Leon,[5] Barbara Leuchs,[20] Gabriele Lux,[21] Catherine Melas,[12,13] Hiroaki Mizukami,[22] Philippe Moullier,[7] Marcus Müller,[20] Keiya Ozawa,[22] Tina Philipsberg,[10] Karine Poulard,[16] Christina Raupp,[20] Christel Rivière,[16] Sigrid D. Roosendaal,[23] R. Jude Samulski,[6] Steven M. Soltys,[6] Richard Surosky,[24] Liliane Tenenbaum,[12,13] Darby L. Thomas,[25] Bart van Montfort,[23] Gabor Veres,[25] J. Fraser Wright,[26,27] Yili Xu,[24] Olga Zelenaia,[26] Lorena Zentilin,[19] and Richard O. Snyder[8,9,28]

Abstract

A recombinant adeno-associated virus serotype 2 Reference Standard Material (rAAV2 RSM) has been produced and characterized with the purpose of providing a reference standard for particle titer, vector genome titer, and infectious titer for AAV2 gene transfer vectors. Production and purification of the reference material were carried out by helper virus–free transient transfection and chromatographic purification. The purified bulk material was vialed, confirmed negative for microbial contamination, and then distributed for characterization along with standard assay protocols and assay reagents to 16 laboratories worldwide. Using statistical transformation and modeling of the raw data, mean titers and confidence intervals were determined for capsid particles ({X}, 9.18×10^{11} particles/ml; 95% confidence interval [CI], 7.89×10^{11} to 1.05×10^{12} particles/ml), vector genomes ({X}, 3.28×10^{10} vector genomes/ml; 95% CI, 2.70×10^{10} to 4.75×10^{10} vector genomes/ml), transducing units

[1]Gene Therapy Program, Department of Pathology and Laboratory Medicine, University of Pennsylvania, Philadelphia, PA 19104.
[2]Department of Epidemiology and Health Policy Research, University of Florida College of Medicine, Gainesville, FL 32610.
[3]Medical Genetics, Department of Pediatrics, Federico II University, 80131 Naples, Italy.
[4]Telethon Institute of Genetics and Medicine (TIGEM), 80131 Naples, Italy.
[5]Center of Animal Biotechnology and Gene Therapy and Department of Biochemistry and Molecular Biology, School of Veterinary Medicine, Universitat Autònoma de Barcelona, 08193-Bellaterra, Spain.
[6]Gene Therapy Center, University of North Carolina at Chapel Hill, Chapel Hill, NC 27599.
[7]INSERM UMR649, Centre Hospitalier Universitaire de Nantes, 44007 Nantes, France.
[8]Center of Excellence for Regenerative Health Biotechnology, University of Florida, Gainesville, FL 32611.
[9]Division of Cellular and Molecular Therapy, Department of Pediatrics, University of Florida, Gainesville, FL 32610.
[10]Powell Gene Therapy Center Vector Core, University of Florida, Gainesville, FL 32611.
[11]Molecular Physiology and Therapeutics Branch, National Institute of Dental and Craniofacial Research, National Institutes of Health, Bethesda, MD 20892.
[12]Laboratory of Experimental Neurosurgery, Free University of Brussels, 1070 Brussels, Belgium.
[13]Multidisciplinary Research Institute, Free University of Brussels, 1070 Brussels, Belgium.
[14]Center for Gene Therapy, Research Institute at Nationwide Children's Hospital, Columbus, OH 43205.
[15]Department of Pediatrics, Ohio State University, Columbus, OH 43210.
[16]Généthon, 91000 Evry, France.
[17]Gene Therapy Center, University of Massachusetts Medical School, Worcester, MA 01655.
[18]Department of Pediatrics, University of Massachusetts Medical School, Worcester, MA 01655.
[19]Molecular Medicine Laboratory, International Center for Genetic Engineering and Biotechnology (ICGEB), 34149 Trieste, Italy.
[20]Infection and Cancer Program, German Cancer Research Center, 69120 Heidelberg, Germany.
[21]Pharmazeutische Fabrik Dr. Reckeweg, 64625 Bensheim, Germany.
[22]Division of Genetic Therapeutics, Center for Molecular Medicine, Jichi Medical University, Shimotsuke 329-0498, Japan.
[23]Amsterdam Molecular Therapeutics, 1100 Amsterdam, The Netherlands.
[24]Sangamo BioSciences, Richmond, CA 94804.
[25]Applied Genetic Technologies, Alachua, FL 32615.
[26]Center for Cellular and Molecular Therapeutics, Children's Hospital of Philadelphia, Philadelphia, PA 19104.
[27]Department of Pathology and Laboratory Medicine, University of Pennsylvania School of Medicine, Philadelphia, PA 19104.
[28]Department of Molecular Genetics and Microbiology, University of Florida College of Medicine, Gainesville, FL 32610.

({X}, 5.09×10^8 transducing units/ml; 95% CI, 2.00×10^8 to 9.60×10^8 transducing units/ml), and infectious units ({X}, 4.37×10^9 $TCID_{50}$ IU/ml; 95% CI, 2.06×10^9 to 9.26×10^9 $TCID_{50}$ IU/ml). Further analysis confirmed the identity of the reference material as AAV2 and the purity relative to nonvector proteins as greater than 94%. One obvious trend in the quantitative data was the degree of variation between institutions for each assay despite the relatively tight correlation of assay results within an institution. This relatively poor degree of interlaboratory precision and accuracy was apparent even though attempts were made to standardize the assays by providing detailed protocols and common reagents. This is the first time that such variation between laboratories has been thoroughly documented and the findings emphasize the need in the field for universal reference standards. The rAAV2 RSM has been deposited with the American Type Culture Collection and is available to the scientific community to calibrate laboratory-specific internal titer standards. Anticipated uses of the rAAV2 RSM are discussed.

Introduction

Recombinant adeno-associated viral (rAAV) vectors are rapidly becoming the gene delivery vehicle of choice for gene transfer, with numerous publications describing their use in animal models and more recently in clinical trials (Warrington and Herzog, 2006; Mueller and Flotte, 2008). The movement of the gene therapy field toward the use of rAAV vectors in clinical trials is largely due to the demonstration of long-term transgene expression in animal models with little associated toxicity and good overall safety profiles in humans (Snyder and Flotte, 2002; Moss *et al.*, 2004; Warrington and Herzog, 2006; Maguire *et al.*, 2008; Mueller and Flotte, 2008; Brantly *et al.*, 2009). Most of the historic data involve rAAV serotype 2 vectors, but vector systems based on other AAV serotypes with more efficient gene delivery profiles in specific tissues are currently in human trials (Brantly *et al.*, 2009; Nienhuis, 2009) and their use will likely increase.

A major problem associated with the body of data to date has been the inability to normalize vector doses administered by different investigators to animals and humans. Thus, there is a need for a reference standard that is recognized by the rAAV research community and that is used to normalize laboratory-specific internal reference standards and test vector titers related to common reference standard units. This need is not new to the field of gene therapy and has previously been addressed for adenoviral vectors. The Adenovirus Reference Material Working Group (ARMWG) developed and characterized the adenovirus reference material (ARM) for the purpose of normalizing titers and doses of gene therapy vectors based on adenovirus type 5 (Hutchins, 2002). Following this example, the U.S. Food and Drug Administration (FDA) and the National Institutes of Health (NIH) Recombinant DNA Advisory Committee (RAC), together with the support of the National Gene Vector Laboratory (NGVL), a program of the NIH National Center for Research Resources (NCRR), encouraged academic and industry scientists within the AAV community to form an AAV Reference Standard Working Group (AAVRSWG) charged with the development a high-quality rAAV reference standard material (Snyder and Flotte, 2002). The AAVRSWG is a volunteer organization and comprises members from both industry and universities in nine different countries, and the International Society for BioProcess Technology (www.ISBioTech.org), under the guidance of the FDA and NIH (Moullier and Snyder, 2008; Potter *et al.*, 2008). Although new serotypes of AAV are currently emerging as efficient gene delivery vectors, the AAVRSWG decided that the first AAV reference standard material should be based on the prototypical AAV serotype 2 because this is by far the best characterized serotype. The approach used in the development of this reference standard lays the groundwork for the development of reference standard materials based on other serotypes. Indeed, a second AAVRSWG has been formed for the development of an AAV8 reference material (Moullier and Snyder, 2008).

The AAV2RSWG recognized that the rAAV2 reference standard material (rAAV2 RSM) must be supplied in sufficient quantity to each requestor for use in all necessary tests at each location, be of high quality, and remain stable for an extended period of time. The group drew up guidelines for the production and purification of the rAAV2 RSM, which were carried out at the Vector Core of the University of Florida's Powell Gene Therapy Center (Gainesville, FL) (Potter *et al.*, 2008). The production process involved cotransfection of batches of ten 10-layer Cell Factories containing HEK293 cells with an AAV2 genome/eGFP transgene plasmid and a second plasmid encoding the AAV2 capsid proteins and necessary helper functions. The transfected cells were harvested and the vector was purified by sequential rounds of column chromatography. A Quality Control subcommittee of the AAV2RSWG was formed for the purpose of characterizing the rAAV2 RSM. In consultation with members of the AAV2RSWG, the committee selected the following characterization assays: (1) capsid titer by A20 enzyme-linked immunosorbent assay (ELISA; Progen Biotechnik, Heidelberg, Germany); (2) vector genome titer by quantitative polymerase chain reaction (qPCR); (3) infectious titer by median tissue culture infective dose ($TCID_{50}$) with qPCR readout and by transduction (green fluorescent protein [GFP] readout); and (4) purity and capsid identification by sodium dodecyl sulfate–polyacrylamide gel electrophoresis (SDS–PAGE).

The AAV2 RSM was distributed worldwide to 16 laboratories that volunteered to conduct one or more of the characterization assays. Testing proceeded from July 2008 to March 2009, at which point the quantitative data were collated and statistically analyzed to determine mean titer and confidence intervals. Preliminary analysis showed significant variance and nonnormal data distribution with all of the assays except for particle titer determination. The variance was observed despite providing a standardized protocol and reagents to the testing group and highlights the need within the AAV community for a reference standard with which

assay titers can be normalized. Using statistical transformation to better approximate normal distributions and modeling to offset the lack of independence of duplicate assays within an institution, appropriate estimations of the mean titers and confidence intervals have been determined.

Materials and Methods

Reference standard material production

Production and purification of the rAAV2 RSM were carried out at the Vector Core of the University of Florida's Powell Gene Therapy Center between February 2006 and January 2007. The production process has been described in detail elsewhere (Potter *et al.*, 2008) and is briefly summarized here. Production was initiated by cotransfection of HEK293 cells in ten 10-layer Nunc Cell Factories (Thermo Fisher Scientific, Waltham, MA) with plasmid pTR-UF-11, containing the vector genome and eGFP expression cassette (Burger *et al.*, 2004), and the pDG-KanR helper plasmid, a kanamycin-resistant version of pDG (Grimm *et al.*, 1998) at a 1:1 molar ratio, using a calcium phosphate precipitation method. After a 60-hr incubation at 37°C, 5% CO_2, transfected cells were washed with phosphate-buffered saline (PBS) and harvested in PBS containing 5 m*M* EDTA. Samples of cells were combined with spent tissue culture medium and tested for mycoplasma and *in vitro* adventitious agents. Cells were collected by centrifugation and stored at −20°C until purified. For vector purification, cells were thawed, lysed with 0.5% sodium deoxycholate, treated with Benzonase (Merck, Darmstadt, Germany), and then disrupted by microfluidization. Virions were then purified by STREAMLINE (GE Healthcare Life Sciences, Piscataway, NJ) heparin affinity chromatography. Peak fractions were pooled and applied to a Phenyl Sepharose (GE Healthcare Life Sciences) chromatography column. The flow-through collected from this second purification step was purified and concentrated by sulfopropyl cation-exchange chromatography. Vector was eluted with 5–10 ml of 135 m*M* NaCl in PBS (equivalent to 285 m*M* ionic strength) and stored at −80°C. Eighteen batches were prepared and pooled. The purified bulk was diluted to $\sim 2\times10^{11}$ vector genomes (VG)/ml with 135 m*M* NaCl in PBS, and sterile filtered into two 1.3-liter portions. This filtered formulated bulk was stored frozen (–80°C) until vialed. One of the 1.3-liter portions of the bulk was thawed and refiltered, and 0.5 ml was dispensed into 2087 vials at the American Type Culture Collection (ATCC, Manassas, VA) to produce VR-1616, the rAAV2 RSM.

Predistribution testing

Mycoplasma. Mycoplasma testing of the production culture cell harvest and of the filtered formulated bulk purified material was performed at a contract testing laboratory (WuXi AppTec, Shanghai, China). For the cell harvest material, medium and supernatant from each production batch were sampled and pooled for testing. A total of 1×10^7 cells in 15 ml of production culture supernatant was tested according to Good Laboratory Practice (GLP), using the "Points to Consider" assay described by the FDA Center for Biologics Evaluation and Research (CBER/FDA, 1993). This assay detects the presence of mycoplasma by both indirect (cell culture) and direct (broth and agar) assays. The test article was incubated with monkey kidney cells, stained with a DNA-binding fluorochrome (Hoechst stain), and evaluated microscopically by epifluorescence. Agar and broth flasks were inoculated with test article and incubated anaerobically and aerobically, respectively. Broths were subcultured onto agar plates on days 3, 7, and 14 days postinoculation. All plates were examined no sooner than 14 days postinoculation. Purified bulk rAAV2 RSM was tested by a modification of the "Points to Consider" assay, in which three cycles of inoculation and incubation on Vero cells precede the assay to allow amplification of mycoplasma. Both harvested material and purified bulk material were also tested, using a PCR assay directed against the 16S rRNA gene of various mycoplasma species (WuXi AppTec).

Bioburden. The presence of aerobes, fungi, spores, and anaerobes in the purified bulk material was quantified by plating on various media under specific incubation conditions (WuXi AppTec). The sensitivity of this assay is <5 colony-forming units (CFU)/ml.

Sterility. The vialed rAAV2 RSM (cat. no. VR-1616; ATCC) was tested for sterility at the Indiana University Vector Production Facility (Indianapolis, IN) according to GLP guidelines. The presence of aerobes, anaerobes, and fungi was tested by direct inoculation of thioglycolate broth, Trypticase soy broth, and Sabouraud dextrose agar and incubation for 14 days at the appropriate temperature. Negative and positive (*Bacillus subtilis*, *Candida albicans*, and *Bacteroides vulgatus*) controls were included.

Endotoxin. The vialed rAAV2 RSM was also tested for endotoxin at the Indiana University Vector Production Facility according to GLP guidelines and using the *Limulus* amebocyte lysate gel-clotting assay. Test samples were assayed in duplicate and diluted 2-fold with water. The test reagent (100 μl) was added to the rAAV2 RSM dilution and incubated at 37°C for 60 min, and the tube was examined for the presence of a gel clot. Negative, positive, and spiked controls were included. The sensitivity of the assay was 0.06 endotoxin unit (EU)/ml.

Previaling stability study. An rAAV2-GFP vector preparation at 2×10^{11} VG/ml, in the same formulation as the rAAV2 RSM (PBS + 135 m*M* NaCl), was placed in polypropylene and glass vials (not siliconized) at 0.5 ml per vial. Vials of each type were stored at both temperatures. Vials held at room temperature were assayed for infectious titer after 1 hr, 1 day, 3 days, and 7 days; vials stored at −80°C were assayed for infectious titer at 1 hr, 1 day, 14 days, 35 days, and 124 days (Potter *et al.*, 2008).

RSM handling stability study. The rAAV2 RSM was thawed on ice and aliquoted into siliconized plastic vials. Aliquots were either tested immediately for transducing titer, infectious titer, and vector genome titer or stored at 4°C or −80°C for 3 days and then tested.

rAAV2 RSM handling. For AAV2 RSM characterization, each testing laboratory received two vials from the ATCC on dry ice. On receipt both vials were stored frozen at −70°C to −90°C. One vial was thawed at room temperature while

mixing gently and then kept on wet ice. Within 1 hr of thawing, the infectious titer and transducing titer assays were conducted. The remainder of the thawed vial was stored at 4°C and mixed gently on use. Within 5 days of vial thaw, the particle titer, vector genome titer, and purity/identity assays were performed. These steps were repeated for the second vial, starting on a different calendar day.

rAAV2 RSM characterization assays

Brief descriptions of each characterization assay follow. For those wishing to reproduce these assays, detailed protocols can be found at the links specified below or may be requested directly from M. Lock or R. Snyder.

Particle titer. Particle concentration was determined by each laboratory, using four separate dilution series from a single vial in the Progen AAV2 titration ELISA (cat. no. PRATV; Progen Biotechnik), by comparison with a standard curve prepared from a previously titered rAAV2 preparation. See the protocol posted at http://www.isbiotech.org/ReferenceMaterials/pdfs/AAV2_capsid_titer_assay_V2.pdf

Vector genome titer. Vector genome concentration was determined in duplicate, testing one replicate from each of two vials, by quantitative PCR of serial dilutions of rAAV2 RSM against a standard curve of plasmid pTR-UF-11 (MBA-331; ATCC) (Burger *et al.*, 2004) See the protocol posted at http://www.isbiotech.org/ReferenceMaterials/pdfs/AAV2_RSS_genome_copy_titration_QPCR.pdf

Transducing titer. Serial 10-fold dilutions of rAAV2 RSM were made on HeLaRC32 cells (CRL-2972; ATCC) (Chadeuf *et al.*, 2000) and coinfected with adenovirus type 5 (VR-1516; ATCC). Fluorescence microscopy was used to count GFP-expressing cells at 72 hr postinfection. See the protocol posted at http://www.isbiotech.org/ReferenceMaterials/pdfs/AAV2_RSS_Infectious_titer_assays_V2.pdf

Infectious titer. Serial 10-fold dilutions of an rAAV2 reference standard stock (RSS) were made on HeLaRC32 cells (CRL-2972; ATCC) and coinfected with adenovirus type 5 (VR-1516; ATCC). Seventy-two hours postinfection total cell DNA was extracted and analyzed for vector genome copies by qPCR. Input vector genomes were subtracted and $TCID_{50}$ titers were calculated according to the method of Kärber (Kärber, 1931). See the protocol posted at http://www.isbiotech.org/ReferenceMaterials/pdfs/AAV2_RSS_Infectious_titer_assays_V2.pdf

Purity and identity. The purity and identity of the rAAV2 RSM were evaluated by SDS–PAGE, using SYPRO ruby (Invitrogen, Carlsbad, CA) or silver staining (SilverXpress; Invitrogen). The AAV2 VP1, VP2, and VP3 capsid protein bands were evaluated for their stoichiometry and size. Purity relative to nonvector impurities visible on stained gels was determined. Vector identity was verified by observation of the electrophoretic banding pattern expected for AAV2 and by comparison with positive controls. See the protocol posted at http://www.isbiotech.org/ReferenceMaterials/pdfs/AAV2_RSS_Identity-Purity_assay.pdf

Results

rAAV2 RSM production and predistribution testing

The goal of the AAV2RSWG manufacturing subcommittee was to make a single lot of an rAAV-eGFP vector with a yield of 1×10^{15} vector genomes. Eighteen batches of ten 10-layer cell factories containing 293 cells were transfected and the resulting AAV vector was purified from the transfected cells by sequential heparin affinity, hydrophobic interaction, and cation-exchange chromatography. The final column eluates from the 18 batches prepared were pooled for a total of 150 ml. The genome titer of this purified bulk was assayed by dot–blot assay and, using this method, it was determined that the material contained 5.69×10^{14} VG (Potter *et al.*, 2008). The purified bulks were combined, diluted to $\sim2\times10^{11}$ VG/ml, and sterile filtered into two 1.3-liter portions. This filtered formulated bulk was stored frozen (–80°C) in anticipation of vialing. In March 2008, one of the 1.3-liter portions of the bulk stock was thawed, refiltered, and dispensed into 2087 vials at the ATCC to produce the rAAV2 RSM (cat. no. VR-1616). The vials, frozen in the repository at the ATCC, are available for distribution. The other 1.3-liter portion of the bulk material remains frozen at the ATCC, to be dispensed at a later date if demand warrants (Potter *et al.*, 2008).

Before freezing, the filtered formulated bulk was sampled (5 ml) and tested for bioburden by a contract testing laboratory (WuXi AppTec). Aerobes, fungi, spores, and obligate anaerobes all tested negative with an assay sensitivity of <5 CFU/sample. Before distribution, the vialed rAAV2 RSM was tested under GLP guidelines for sterility (aerobes, anaerobes, fungi) and endotoxin at the Indiana University Vector Production Facility. No bacterial or fungal contamination was detected and endotoxin levels were less than 0.06 EU/ml. The production culture cell harvest and the filtered purified bulk material were tested at WuXi AppTec for mycoplasma contamination as detailed in Materials and Methods (GLP "Points to Consider" assay). The harvest material tested positive for *Mycoplasma arginini* (bovine origin) and the tests were valid (i.e., all controls performed). The filtered purified bulk material was tested for mycoplasma, using a modified assay with increased sensitivity. In this test, a sample of the bulk material was passaged three times on Vero cells before performing the GLP "Points to Consider" assay. The bulk material tested negative for mycoplasma whereas the spike-in controls performed as expected, indicating that the assay was valid. Last, the harvest and bulk materials were tested by PCR (WuXi AppTec) for a 16S rRNA gene region specific to various mycoplasma species. Using this assay, the harvest was confirmed positive and the filtered formulated bulk again tested negative, with all controls performing as expected. Thus whereas the harvested cells were positive for mycoplasma, the purified bulk was negative for viable mycoplasma and no mycoplasma DNA was detected, so it was concluded that the purification process likely separated and/or inactivated the contaminating mycoplasma present in the harvest material (Potter *et al.*, 2008).

Beta testing

The AAV2RSWG Quality Control subcommittee was formed for the purpose of characterizing the rAAV2 RSM.

Table 1. rAAV2 Reference Standard Material Testing Laboratories

University of Naples Federico II, Italy
University of North Carolina Vector Laboratories, USA
Universitat Autònoma de Barcelona, Spain
Research Institute at Nationwide Children's Hospital, USA
University of Florida, USA
Laboratoire de Thérapie Génique, France
Généthon, France
Applied Genetic Technologies, USA
International Center for Genetic Engineering and Biotechnology (ICGEB), Italy
German Cancer Research Center (DKFZ), Germany
University of Pennsylvania, USA
Jichi Medical University, Japan
Sangamo BioSciences, USA
Université Libre de Bruxelles, Belgium
Amsterdam Molecular Therapeutics, The Netherlands
Children's Hospital of Philadelphia, USA

Decisions regarding the characterization assays required were made in consultation with the AAV2RSWG, and members were invited to submit their assay protocols. These protocols were reviewed and a lead protocol was chosen for each assay. The assays chosen included (1) confirmation of the serotype and capsid particle titer by A20 ELISA (Progen Biotechnik); (2) determination of vector genome titer by qPCR; (3) determination of infectious titer by median tissue culture infective dose ($TCID_{50}$) with qPCR readout and by transduction (GFP readout); (4) evaluation of the purity, capsid subunit stoichiometry, and chemical integrity of the capsid by SDS–PAGE.

During the protocol selection process it was realized that the highest level of assay reproducibility in the various testing laboratories could be ensured only if certain reagents were provided along with the rAAV2 RSM. The reagents, which are now available from the ATCC, include a cell line expressing the AAV2 *rep* and *cap* genes (HeLa32; kindly provided by P. Moullier, INSERM UMR649 Nantes, France), a concentrated adenovirus helper virus (the adenovirus type 5 reference standard material, ARM) (VR-1516; ATCC) for the transduction and infectivity assays, and the pTR-UF-11 vector plasmid (kindly provided by S. Zolotukhin, Powell Gene Therapy Center and Division of Cellular and Molecular Therapy, Department of Pediatrics, University of Florida, Gainesville, FL) used to manufacture the AAV2 RSM viral vector. For both genome titer and infectious titer assays, a qPCR primer–probe set directed to the simian virus 40 (SV40) poly(A) sequence and a dilution series specific to the RSM were selected. For the purity and identity assay, commercially available assay reagents with the highest sensitivity were suggested. Using these reagents, the modified assay protocols were beta tested at the University of Pennsylvania Gene Therapy Program against both in-house standards (AAV2.CMV.eGFP and AAV2.CMV.lacZ) and the rAAV2 RSM itself. The genome, infectious, and transduction titers of the in-house standards correlated well with the titers previously established by in-house assays (see Table 2; and data not shown) and vector genome-to-infectious or transduction unit ratios were similar to those published elsewhere (Salvetti *et al.*, 1998; Zolotukhin *et al.*, 1999; Zen *et al.*, 2004). Repeating the beta testing with the rAAV2 RSM allowed appropriate dilution ranges to be established for several of the characterization assays. The finalized protocols were posted at the International Society for BioProcess Technology website (www.ISBioTech.org) and the HeLaRC32 cells (CRL-2972; ATCC), pTR-UF-11 plasmid (MBA-331; ATCC), and ARM (VR-1516; ATCC) assay reagents were made available through the ATCC. The rAAV2 RSM (VR-1616; ATCC) was distributed along with the required reagents and handling instructions to 16 laboratories worldwide (Table 1) that volunteered to conduct one or more of the characterization assays.

Before filling the rAAV2 RSM, a study was conducted with a different lot of rAAV2-GFP vector in the same formulation to evaluate the short-term stability of the vector at room temperature (the filling condition) and at −80°C (the storage condition). Vials were filled with the beta test vector and held at the test temperatures for the time periods indicated (see Materials and Methods) and were then assayed for infectious titer. In all scenarios, a 30–40% drop was observed between the initial titer and the average of all samples taken during the time course and it was assumed that this loss likely indicated absorption to the container surfaces at the low vector concentration (Potter *et al.*, 2008), because these containers were not siliconized. After filling the rAAV2 RSM, a limited study was also conducted to evaluate the stability of the rAAV2 RSM after post-thaw storage at 4°C, and after refreezing at −80°C. The purpose of the study was to determine the appropriate conditions for handling of the RSM once received by the testing laboratory. Transduction titers fell 35 and 56% after storage or refreezing at 4°C and −80°C, respectively, and infectious titer fell 78 and 63%, respectively

Table 2. Qualification of Reference Standard Material (RSM) Testing Methods Using In-House Standards and Beta Testing of rAAV2 RSM Under Various Storage Conditions

	In-house standards		*rAAV2 RSM*		
	AAV2.CMVe.GFP	*AAV2.CB.lacZ*	*At thaw*	*4°C*[a]	*−80°C*[a]
Transducing titer (GFU/ml)	1.42×10^{10}	NA	1.89×10^{9}	1.23×10^{9}	8.38×10^{8}
Infectious titer ($TCID_{50}$ IU/ml)	6.96×10^{10}	2.42×10^{11}	1.65×10^{10}	3.56×10^{9}	6.23×10^{9}
Physical titer (vector genomes/ml)	4.53×10^{12}	2.15×10^{12}	3.39×10^{10}	3.39×10^{10}	3.41×10^{10}
Vector genomes: infectious units	65	8.87	2.05	9.53	5.39
Vector genomes: transducing units	319	NA	17.90	27.50	40.70

Abbreviations: GFU, GFP (green fluorescent protein) forming units; NA, not available; $TCID_{50}$, median tissue culture infective dose.
[a]Assayed 3 days postthawing, after storage at the indicated temperature.

(Table 2). Conversely, no change was observed in the vector genome titers under the various storage conditions. These results indicated that the postthaw storage conditions were adversely affecting the potency of the rAAV2 RSM and that this decrease was not due to absorption to the siliconized aliquot vials used in this study, because the vector genome titer was unchanged. On the basis of these data the decision was made to test two separate aliquots of the RSM and to determine transducing and infectious titers within 1 hr of thawing a vial.

rAAV2 RSM characterization

The characterization phase of the rAAV2 RSM proceeded from July 2008 to March 2009. On receipt, the RSM was evaluated by the 16 testing laboratories according to the posted protocols, and data were recorded on the assay worksheets provided, which contained the necessary calculations for titer determination. Fifteen laboratories performed the particle titer assay (31 replicates), 16 laboratories performed the genome titer assay (36 replicates), 10 laboratories performed the infectious titer assay (23 replicates), and 12 laboratories performed the transducing titer assay (19 replicates). In some cases (four of the tests), substantial experimental deviation from the posted protocols was noted and these data have been omitted from the statistical analyses.

The raw data that emerged from the testing laboratories for the four quantitative titer assays (Table 3) was statistically analyzed to determine true mean titer values and confidence intervals. The distribution was first visualized as histograms (Fig. 1), and it was noted that with the possible exception of the particle titer results, the data do not appear to be nor-

TABLE 3. rAAV2 REFERENCE STANDARD MATERIAL RAW CHARACTERIZATION DATA

Laboratory	*Replicate*	*Particle titer (ELISA) (pt/ml)*	*Genome titer (qPCR) (VG/ml)*	*Transducing titer (green cells) (GFU/ml)*	*Infectious titer (TCID50) (IU/ml)*[a]
A	1	1.08×10^{12}	4.68×10^{10}	1.27×10^{9}	
	2	1.26×10^{12}	8.77×10^{10}	1.26×10^{9}	
B	1	8.25×10^{11}	7.03×10^{10}	3.63×10^{8}	6.32×10^{9}
	2	8.28×10^{11}	7.58×10^{10}	1.00×10^{8}	1.36×10^{9}
	3		9.39×10^{10}	7.15×10^{7}	2.00×10^{9}
C	1	7.70×10^{11}	8.60×10^{10}	9.80×10^{6}	
	2	6.05×10^{11}	4.19×10^{10}		
D	1	8.80×10^{11}	1.01×10^{10}	1.70×10^{9}	1.02×10^{10}
	2	7.83×10^{11}	3.71×10^{10}	2.77×10^{9}	6.96×10^{9}
E	1	1.16×10^{12}	1.58×10^{10}		
	2	1.04×10^{12}	1.14×10^{10}		
	3		1.61×10^{10}		
F	1	1.66×10^{12}	2.17×10^{10}	6.60×10^{8}	
	2	1.01×10^{12}	2.12×10^{10}	5.70×10^{8}	
G	1	1.90×10^{12}	1.13×10^{10}	4.02×10^{8}	3.23×10^{9}
	2	9.39×10^{11}	1.30×10^{10}		2.67×10^{9}
H	1		2.04×10^{10}		
	2		2.13×10^{10}		
I	1	8.56×10^{11}	5.93×10^{10}	2.20×10^{7}	
	2	7.08×10^{11}	6.10×10^{10}	2.95×10^{7}	
J	1	1.24×10^{12}	3.39×10^{10}	1.89×10^{9}	1.65×10^{10}
	2	1.07×10^{12}	4.49×10^{10}	1.22×10^{9}	2.42×10^{10}
K	1	5.29×10^{11}	3.72×10^{10}	2.01×10^{8}	
	2	7.75×10^{11}	3.62×10^{10}	2.04×10^{8}	
L	1	8.13×10^{11}	1.31×10^{9}	5.96×10^{8}	1.50×10^{9}
	2	4.99×10^{11}	1.63×10^{10}	6.48×10^{8}	6.96×10^{8}
M	1	1.11×10^{11}	1.16×10^{10}	8.88×10^{8}	2.00×10^{9}
	2	1.25×10^{11}	1.53×10^{10}	4.52×10^{8}	1.50×10^{9}
N	1	3.93×10^{11}	1.47×10^{10}	3.82×10^{8}	2.00×10^{10}
	2	5.59×10^{11}	7.63×10^{9}	2.62×10^{8}	7.66×10^{9}
	3	9.58×10^{11}	4.24×10^{9}		2.40×10^{9}
O	1	1.06×10^{12}	6.04×10^{10}		
	2	1.09×10^{12}	1.27×10^{11}		
P	1	8.02×10^{11}	4.20×10^{10}		7.66×10^{9}
	2	7.74×10^{11}	5.10×10^{10}		6.96×10^{9}
	3		4.82×10^{10}		9.28×10^{9}
Mean		9.43×10^{11}	3.82×10^{10}	6.94×10^{8}	7.00×10^{9}
Standard deviation		3.19×10^{11}	2.97×10^{10}	7.03×10^{8}	6.70×10^{9}

[a]Four replicate test results were omitted because of documented experimental deviation from the posted protocols.